Psychiatry Research: Neuroimaging 359 (2026) 112205

Contents lists available at ScienceDirect

Psychiatry Research: Neuroimaging

journal homepage: www.elsevier.com/locate/psychresns

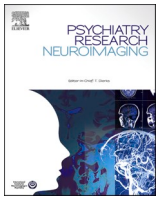

Attentional bias to death-related stimuli: Modeling cortical dynamics underlying suicide risk

Yoojin Lee [a], Jessica R. Gilbert [a], Steven J. Lamontagne [a], Halla F. Hafermann [a], Laura R. Waldman [a], Megan S. Kenna [b], Nancy E. Adleman [c], David A. Jobes [c], Carlos A. Zarate Jr. [a], Elizabeth D. Ballard [a,*]

[a] Experimental Therapeutics and Pathophysiological Branch, National Institutes of Mental Health, National Institutes of Health, Bethesda, MD, USA
[b] Mindmap Private Psychological Practice, Washington, DC, USA
[c] Department of Psychology, The Catholic University of America, Washington, DC, USA

ARTICLE INFO

Keywords:
Magnetoencephalography (MEG)
Suicide
Dynamic causal modeling
DCM
Life/death dot-probe
Attentional bias

ABSTRACT

This study used magnetoencephalography (MEG) and the life/death dot-probe task to investigate neural correlates of suicide risk, specifically whether suicide risk moderates selective attention to death-related cues. Three groups were examined: individuals with a lifetime history of suicide attempt or ideation (suicide risk; $n = 17$); those with depression but no suicide risk (clinical controls; $n = 17$); and healthy volunteers ($n = 19$). Individuals with suicide risk exhibited decreased activity in the superior parietal lobule (SPL), entorhinal cortex (EC), and middle temporal gyrus (MTG) in the death and incongruent conditions across multiple bandwidths ($ps < 0.05$), indicating suicide risk-associated dysregulation of brain regions related to signal processing. Dynamic causal modeling was used to estimate effective connectivity. In the death condition, reduced feedforward connectivity was observed from the early visual cortex to the EC, then to the SPL, and finally to the MTG in the suicide risk group (posteriorps > 0.90), suggesting potential deficits in updating sensory inputs and regulating selective attention. Conversely, in the life condition, reduced connectivity was observed from the MTG to the SPL in the suicide risk group (posteriorps > 0.90), suggesting subtle impairments in downregulating attention orientation during life-related cognitive processes. Abnormalities in selective attention to death-related cues may serve as potential biomarkers for suicide risk.

1. Introduction

Suicide is a significant public health crisis and one of the leading causes of death in the United States (WHO, 2021). Approximately 16 million Americans experience serious thoughts of suicide, a rate that is about 300 times higher than the number of individuals who die by suicide (Substance Abuse and Mental Health Services Administration, 2024). Investigating the etiology and prognosis of suicide risk traditionally relies on self-reports or clinician-administered interviews. In this context, a history of suicide attempts is a recognized risk factor and one of the most validated predictors of future suicidal behaviors (Ryan and Oquendo, 2020). However, self-report and clinician-driven assessments are often compromised by limitations in retrospective memory and fear of stigma, which may inhibit transparent disclosure of suicidal thoughts or behaviors.

Objective measures of suicide risk, such as task-driven responses, offer an alternative for assessing suicide risk factors by evaluating behavioral indicators of risk. For example, such measures can capture high impulsivity, an indicator that confers heightened risk, by measuring poor inhibitory control, impaired cognitive processing, suboptimal decision-making, and deficits in emotional cue processing (Alacreu-Crespo et al., 2020; Bao et al., 2024; Öğüt et al., 2023; Olié et al., 2015; Tsypes et al., 2022). Using task-driven behavioral markers alongside neurobiological biomarkers can augment traditional diagnostic tools for suicide risk and contribute to our understanding of the mechanisms that underlie suicidal behaviors (Lamontagne et al., 2023). Such work may eventually help establish a reliable predictive model of suicidal behaviors, which has largely been unsuccessful to date due to a lack of reliable biomarkers of suicide risk (Large, 2018; Madsen et al., 2017).

* Corresponding author at: Building 10, CRC Room 7-5341, 10 Center Drive, MSC 1282, Bethesda, MD 20892, USA.
E-mail address: Elizabeth.Ballard@nih.gov (E.D. Ballard).

https://doi.org/10.1016/j.pscychresns.2026.112205
Received 21 May 2025; Received in revised form 16 March 2026; Accepted 26 March 2026
Available online 28 March 2026
0925-4927/Published by Elsevier B.V.

Previous research has implicated attentional bias as a marker of suicide risk. Attentional bias refers to an individual's tendency to focus more on one set of stimuli over others (Hamedi et al., 2019). In the context of suicide, attentional bias indicates an increased focus on suicide-related stimuli. For instance, studies have shown that individuals with a history of suicide attempts tend to show increased attentional bias towards suicide-related words or images by taking longer to react to suicide-related cues (Brüdern et al., 2024) or name the colors of suicide-related words (Becker et al., 1999). It is important to note that increased attentional bias appears to be a direct outcome of suicide-related cue processing rather than general processing of negative stimuli (Richard-Devantoy et al., 2016; Tavakoli et al., 2021). This heightened sensitivity to death-related cues is linked to the recurrence of suicide attempts (Cha et al., 2010), indicating its potential relevance within suicide research. A recent study found that individuals at risk for suicide had increased attentional bias to death- or suicide-related words versus healthy volunteers (HVs), as assessed by higher death implicit association test scores and higher suicide interference scores during the death-life implicit association test and the modified Suicide Stroop Task, respectively (Brüdern et al., 2024). However, the difference in attentional bias between those with a past suicide attempt and those with current suicide ideation was minimal, suggesting that attentional bias towards death-related cues may represent a generalized suicide risk. For instance, increased attentional bias could result in insufficient attention or reduced information updating from sensory signals (Becker et al., 1999; Keilp et al., 2008; Li et al., 2021), which may impair perception and produce biased attentional orientation (Patten et al., 2017). Such cognitive patterns could help distinguish suicide risk biologically from disorders such as depression.

Distinct brain regions and networks have been implicated in attentional bias within the context of suicide risk. The prefrontal cortex (PFC), particularly its connectivity to the amygdala, plays a role not only in executive functions such as decision making but also in orienting attention and cognitive reappraisal, both of which are critical for regulating emotion (Dixon and Dweck, 2022; Sequeira et al., 2021; Wang et al., 2024). Reduced PFC activity and quicker responses to emotional stimuli during the Emotional Stroop Task have been observed in individuals at high risk for suicide (Thompson and Ong, 2018), potentially suggesting impulsive decision-making without sufficient emotion regulation. In addition, individuals with depression and a history of suicide attempts showed reduced volumes in both the amygdala and PFC and decreased connectivity between these regions (Wang et al., 2019). The anterior cingulate cortex (ACC) and insula are also associated with suicide risk because their role in emotion processing and interoceptive awareness contribute to attentional bias (Chen et al., 2019; DeVille et al., 2020); however, debates exist regarding the directional nature of these associations (Parisi et al., 2021; Schmaal et al., 2020).

While prior research has focused on emotional processing regions, earlier stages of sensory processing and integration in the brain remain underexplored, as does their relationship to suicide risk. The middle temporal gyrus (MTG), a region involved in multimodal sensory integration (Binder et al., 2009; Calvert and Thesen, 2004; Tzourio et al., 1997), may be a promising target. Hyperactivation of the MTG has been observed in individuals with a history of suicide attempts, and such hyperactivation is associated with increased suicidal thoughts (Chen et al., 2022). In addition, those with a recent suicide attempt have reduced MTG volume (Kim et al., 2021; Peng et al., 2014). Collectively, these findings suggest that MTG dysfunction may lead to insufficient sensory information integration in individuals at risk for suicide. However, the specific mechanisms underlying MTG dysfunction and its implications for attentional bias remain unclear.

Attentional bias can be measured using computerized cognitive tasks, such as the dot-probe task. Studies indicate that individuals with depression exhibit a negative attentional bias on this task, manifested by a preferential focus on negative emotional stimuli (Peckham et al., 2010; Schofield et al., 2012). This bias is associated with a worse prognosis of depression over time (Disner et al., 2017). Interestingly, one study found that attentional bias in depression could be directed towards emotional stimuli regardless of their valence (Trapp et al., 2018), suggesting that the dot-probe task could be used to capture attentional bias towards emotional stimuli, such as happy and angry faces. In the context of suicide risk, there is evidence of attentional bias towards negative emotional stimuli. For instance, children with suicidal thoughts have shown sustained attention towards fearful faces, as measured by prolonged eye-gaze duration (Tsypes et al., 2017). This finding suggests that attentional bias towards negative stimuli may be linked to suicide risk. Notably, a recent study found that young adults with recent suicidal thoughts exhibited facilitated disengagement from suicide-specific stimuli, indicating a non-linear relationship between attentional bias and suicide risk that may be modulated by chronological age (Rosario-Williams and Miranda, 2024). These findings underscore that behavioral results from the dot-probe task alone may not fully explain the mechanisms underlying attentional bias.

In this context, investigating attentional bias towards suicide-related stimuli requires using neuroimaging methods that can capture dynamic, phasic attention processes. Magnetoencephalography (MEG) is uniquely suited for such investigation because it directly measures magnetic fields from neuronal activity with recordings collected at greater than 600 samples per second, providing an immediate reflection of brain function compared to functional magnetic resonance imaging (fMRI) (Hansen et al., 2010) and potentially superior capability for capturing attentional bias. In addition, MEG offers superior temporal resolution to traditional fMRI (Hipp et al., 2012; Toll et al., 2020) and better spatial specificity, with less skull- and scalp-related distortion than other electrophysiological techniques such as electroencephalography (EEG) (Hansen, 2010). This combination of temporal and spatial precision is essential for understanding dynamic neural processes and their dysregulation in individuals at risk for suicide in the context of attentional bias. Interestingly, a previous study found that antidepressant-induced suicidal ideation was associated with decreased transient concordance scores in middle and right frontal regions within theta band (4–8 Hz) EEG power after two days (Hunter et al., 2010), indicating that reduced MEG power in early frequency windows may affect attentional encoding and memory formation in subsequent recognition tasks (Ostrowski and Rose, 2024). This study hypothesized that individuals at risk for suicide would show decreased MEG power in early frequency windows during the dot-probe task.

Dynamic causal modeling (DCM) provides insights into neural connectivity by using a Bayesian framework to fit biophysical models that include equations governing dynamics within and between brain regions to brain imaging data. While DCM has not previously been applied in the context of attentional biases and suicide risk, previous work from our laboratory that used a task measuring implicit suicide biases found that individuals with a recent suicide crisis displayed reduced connectivity between the early visual cortex (VC) and the posterior cingulate cortex during the task (Lamontagne et al., 2023). Moreover, connectivity strength from the early VC to the insula was increased during self-associations with death compared to life. These findings suggest both reduced self-referential processing in those with recent suicide crises and heightened death-related-cue response in general. The findings underscore DCM's potential for exploring neural markers of death-related cue processing.

This study used MEG and the life/death dot-probe task (a modified version of the dot-probe task) to investigate neurophysiological correlates of suicide risk in three groups: individuals with a lifetime history of suicide attempts or ideation; individuals with mood or anxiety disorders but no history of suicidal behaviors to serve as clinical controls; and HVs, defined as individuals with no psychiatric disorder or history of suicidal behaviors. The hypothesis was that, compared to the two other groups, those at greater risk for suicide would demonstrate decreased source-level MEG power in sensory processing brain regions like the MTG

across death, life, congruent, and incongruent conditions during the suicide dot-probe task. DCM was used to investigate effective connectivity among selected brain regions.

2. Methods

2.1. Participants

Fifty-three adults (N = 33F/20 M, mean age: 36.56 ± 13.35 years, range = 20 to 67 years) were recruited through the Neurobiology of Suicide protocol (n = 44; NCT02543983) (Ballard Elizabeth, 2020) or the Development of Imaging Techniques for Studying Mood and Anxiety Disorders protocol (n = 9; NCT00397111) (Fig. 1). Participants were selected and allocated into three groups according to their level of suicide risk. Groups included: (1) individuals with a lifetime history of either suicide attempt or ideation (the suicide risk group (SR); n = 17: 4M/13F; mean age: 36.12 ± 11.36 years); (2) individuals with anxiety or mood disorders but no history of suicide attempts or thoughts (the clinical control group (CC); n = 17: 6M/11F; mean age: 45.44±15.86); and (3) individuals with no history of psychiatric disorders, suicide attempts, or suicidal thoughts (HVs; n = 19: 10M/9F; mean age: 29.00 6.47). Individuals with active suicide risk were managed in the research setting as per our previously published protocol (Ballard Elizabeth, 2020). Psychiatric diagnoses were confirmed by the Structured Clinical Interview for DSM Psychiatric Disorders (SCID) (First, 2002); relevant diagnoses can be found in Table 1. Participants were excluded from the study if they had current drug or alcohol dependence, severe or unstable medical conditions, or tested positive for human immunodeficiency virus. Non-English speakers, pregnant individuals, and individuals with other neurological conditions or schizophrenia were also excluded. The Combined Neuroscience Institutional Review Board approved the protocol at the National Institutes of Health in Bethesda, MD, and all participants provided written, informed consent. Each patient was assigned a Clinical Research Advocate (CRA) from the Human Subjects Protection Unit (HSPU) who acted as an independent advocate from the initial consent phase through completion of the study.

2.2. Clinical scales

Clinician-rated measures of depression and anxiety were assessed using the Montgomery-Åsberg Depression Rating Scale (MADRS) (Montgomery and Asberg, 1979), the 24-item version of the Hamilton Depression Rating Scale (HAMD-24) (Hamilton, 1967), and the Hamilton Anxiety Rating Scale (HAM-A) (Maier et al., 1988). Severity of suicide ideation was assessed using the clinician-rated Scale for Suicide Ideation (SSI) (Beck et al., 1979), which measures past (SSI-Past) and current (SSI-Current) ideation. The mean of the first five items of the SSI-Current was used in analyses (Ballard et al., 2014). Across all scales, higher scores indicate greater impairment. Clinical scales were not available for nine participants in the HV group who were recruited from the Developmental Imaging Techniques for the Mood and Anxiety Disorders protocol (NCT00397111).

2.3. Life/death dot-probe task

The life/death dot-probe task was modified from a previous dot-probe task that used faces as stimuli to identify potential attentional biases between life- and death-related stimuli (Gilbert et al., 2021; Reed et al., 2018) (Fig. 2). First, the layout was redesigned from a horizontal to a vertical format. Second, several words were added to the life, death, and neutral categories. The life/death words were selected from the Death Implicit Association Test (D-IAT) (Cha et al., 2010; Nock et al., 2010). Once the final word lists were compiled, previously developed scales were used to confirm that the life and death words had significantly different valence ratings (indicating word pleasantness) but similar arousal ratings (the degree of arousal prompted by a word) (Warriner et al., 2013). Neutral words differed from both life and death words with regard to both valence (with ratings falling between those of life and death) and arousal (with lower ratings than either life or death words). All three groups of words on average did not differ from each

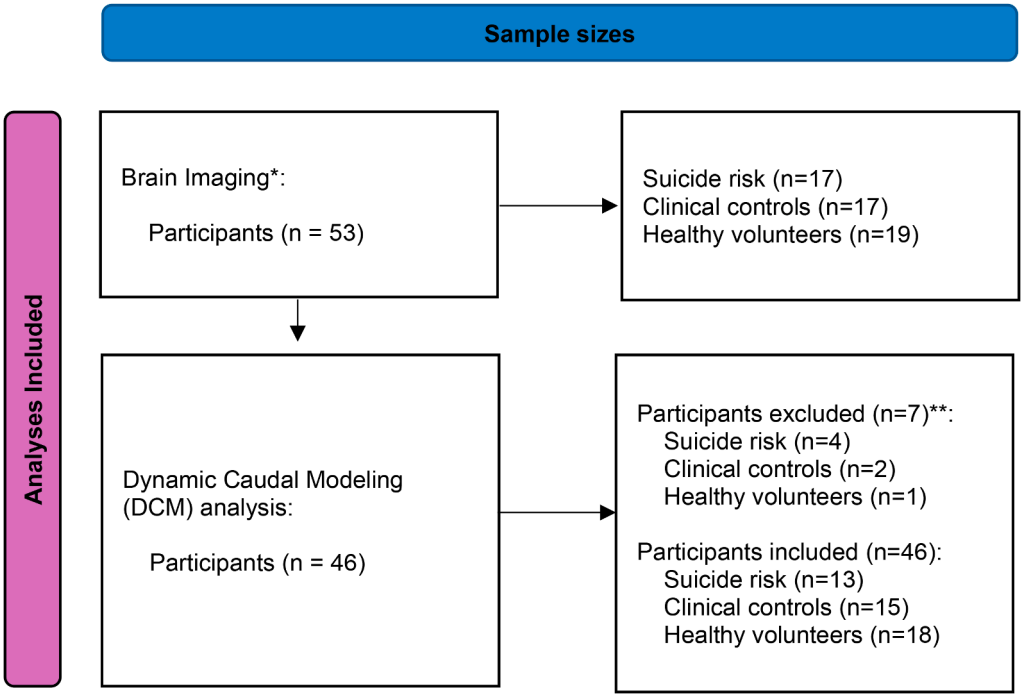

Fig. 1. Sample sizes for the magnetoencephalography (MEG) analysis.
* Participants were included if they underwent task-driven brain imaging using magnetoencephalography (MEG). The group difference analysis was conducted using the participants. **Participants were excluded if individual dynamic causal modeling (DCM) failed to converge due to poor data quality or if fit indices fell more than two standard deviations below the median.

Table 1
Demographic information.

	Suicide risk ($n = 17$)	Clinical controls ($n = 17$)	Healthy volunteers ($n = 19$)	Difference statistics	Explained variance (partial η^2)
Age	36.11 (11.36)	45.44 (15.86)	29.00 (6.47)	$F(2,50) = 8.88$, $p < .001$	0.26
Biological Sex (Female)	13 (76.47%)	11 (68.75%)	9 (47.37%)	$X^2(2) = 3.30$, $p = .192$	
Ethnicity (White)	13 (76.47%)	12 (70.59%)	9 (47.37%)	$X^2(2) = 3.76$, $p = .153$	
Primary Diagnosis (MDD)*	9 (52.94%)	15 (88.24%)	-	$X^2(1) = 3.54$, $p = .060$	
MADRS	20.60 (11.10)	22.80 (9.13)	1.11 (1.36)	$F(2,37) = 18.90$, $p < .001$	0.51
HAMD_24	17.80 (8.90)	19.90 (8.00)	0.78 (1.09)	$F(2,37) = 22.51$, $p < .001$	0.57
HAM-A	11.40 (4.53)	12.60 (4.90)	0.67 (1.00)	$F(2,37) = 26.27$, $p<.001$	0.58
Current Suicide Ideation**	1.75 (2.27)	1.12 (1.78)	-	$F(2,36) = 2.71$, $p = .080$	0.14
Past Suicide Ideation**	25.90 (8.68)	12.30 (9.88)	-	$F(2,29) = 11.80$, $p <.001$	0.43

* In the suicide risk and clinical control groups, anyone not diagnosed with major depressive disorder (MDD) was diagnosed with bipolar disorder.
** Suicide ideation was measured using the Scale for Suicide Ideation (SSI).
MADRS: Montgomery-Åsberg Depression Rating Scale; HAMD-24: Hamilton rating scale for depression with 24 items; HAM-A: Hamilton Anxiety Rating Scale.

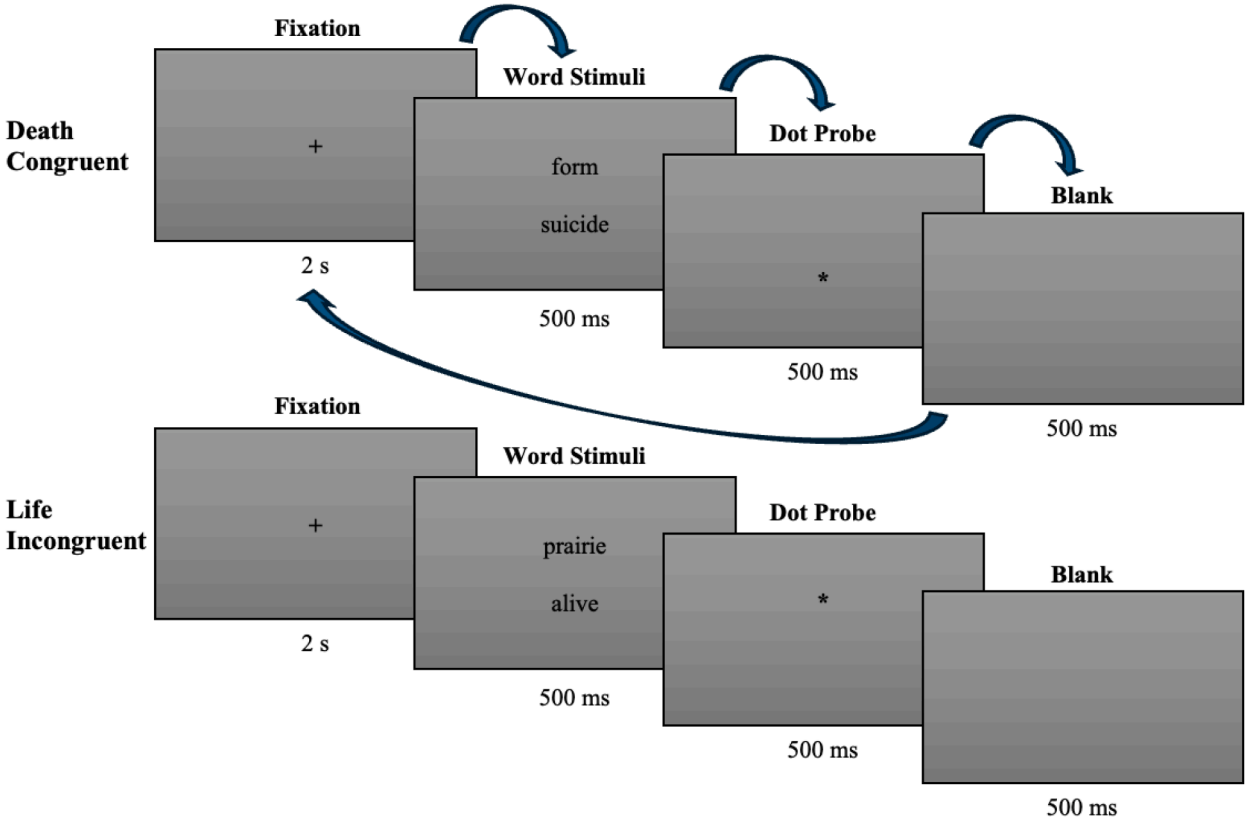

Fig. 2. Design of the suicide-dot-probe task. After a fixation period of two seconds, word stimuli (death-, life-, or neutral-related words) appeared for 500 milliseconds. Subsequently, a dot probe appeared, and the individual responded to its location by directing their attention either to a given word stimulus (i.e., congruent) or a neutral word (i.e., incongruent) over the other for 500 milliseconds. This was followed by a blank screen for 500 milliseconds.

other in terms of word frequency, number of letters, number of syllables, or part of speech according to the Corpus of Contemporary American English (Davies, 2012).

Each participant completed this task in the MEG scanner. As illustrated in Fig. 2, in each trial, participants were first asked to focus on a fixation cross for two seconds. After fixation, participants viewed a pair of words stacked on a screen for 500 ms ($n = 112$ suicide/death-related words, 112 non-suicide/death-related words, and 112 neutral words). Each trial included two words: a neutral word and a target word. The target words were grouped into three categories: life-related, death-related, and neutral. The life/death dot-probe task had three conditions. The first condition paired a life-related word with a neutral word (life trial), the second condition paired a death-related word with a neutral word (death trial), and the third was a control condition consisting of two neutral words (neutral trial). After the words disappeared, a probe briefly (500 ms) flashed in the location of one of the words, and participants used a button box to indicate whether the probe had appeared in either the top or bottom location. Trials were considered congruent if the probe appeared in the location (either top or bottom) of the target word and incongruent if it appeared in the location of the neutral control word.

2.4. MEG processing

Neurophysiological data were collected using a 275-channel CTF MEG system equipped with superconducting quantum interference device-based axial gradiometers (VSM MedTech Ltd., Coquitlam, BC, Canada). Data were recorded at a sampling rate of 1200 Hz and a

bandwidth of 0–300 Hz. MEG data were recorded in a magnetically shielded room, and synthetic third-order balancing was used to actively cancel noise. The MEG data were co-registered to each participant's T1-weighted structural MRI image, obtained from a 3T MRI scanner (3T GE scanner, GE Signa, Milwaukee, WI) using fiducial coils placed at the nasion and the left and right preauricular points. In-house scripts were applied to detect cardiac and muscle artifacts using independent component analysis and manual inspection. Individual spectra were inspected, and trials with visible artifacts (movement, eye blinks) or excessive sensor noise were manually removed. Only artifact-free trials were retained for analysis. Reaction times for the stimuli in the life/death dot-probe task were processed across different conditions: death congruent, death incongruent, life congruent, life incongruent, and neutral. The cleaned data were filtered from 1 to 60 Hz using the SPM12 pipeline and segmented into epochs ranging from -500 to 1500 ms relative to stimulus onset, in bandwidth-specific ranges: theta (4–8 Hz), alpha (9–14 Hz), beta (15–29 Hz), and gamma (30–58 Hz). The epoched MEG data were then source-localized to a 5 mm grid and a 1-second window from the onset of the target stimulus using synthetic aperture magnetometry (Hillebrand et al., 2005) for each condition and frequency band of interest. Statistical maps of group activity were estimated using the linear mixed effects models (*3dLMEr*) in the Analysis of Functional Neuroimages (AFNI) (Chen et al., 2013; Cox, 1996) (see Data Analysis Plan, below). MEG analyses were conducted using the computational resources of the NIH HPC Biowulf cluster (http://hpc.nih.gov).

2.5. Dynamic causal modeling (DCM)

DCM is a generative model that seeks to find hidden neural states from measured brain responses using a Bayesian perspective (Stephan et al., 2010). Individual-level DCM models used the canonical microcircuit framework, a neural mass model that predicts extrinsic effective connectivity among biologically plausible brain regions (Bastos et al., 2012; Pinotsis et al., 2013) through Bayesian inference via the Free Energy Principle (Adams et al., 2016). The DCM model estimates feedforward connectivity, conveying prediction errors (superficial pyramidal cells (SPs) to spiny stellate cells (SSs); SPs to deep pyramidal cells (DPs)) and feedback connectivity conveying top-down suppression (DPs to SPs; DPs to inhibitory interneurons (IIs)). An initial data-driven, hybrid approach (Lee et al., 2024) was used to identify brain regions showing significant group differences in band-specific MEG power analyses. This approach, which ensured capture of all brain regions, showed reduced activity in the SR group compared to other groups, consistent with our hypothesis. Among those brain regions, key regions of interest (ROIs) were selected based on established literature that identified the most biologically plausible pathways for visuospatial attention and contextual processing. Specifically, layered effective connectivity was assessed between four ROIs across conditions: the early VC (Montreal Neurological Institute (MNI) coordinates: $x = -2, y = -88, z = 8$), the superior parietal lobule (SPL; $x = -30$, $y = -66$, $z = 50$), the parahippocampal gyrus/entorhinal cortex (EC; $x = -24$, $y = -8$, $z = -32$), and the MTG ($x = -60$, $y = -14$, $z = -16$). These four regions were selected based on their functions: VC for visual signal input and awareness (Tong, 2003), SPL for attentional control (Corbetta and Shulman, 2002; Hopfinger et al., 2000), EC as a neocortex-hippocampus relay that facilitates memory and learning through synaptic plasticity while integrating sensory information for memory and navigation (Agster and Burwell, 2013; Grande et al., 2022; Yaniv et al., 2003), and MTG for multimodal sensory integration and lexical-syntactic processing (Snijders et al., 2010).

The DCM model explained time-locked, averaged electrophysiological fluctuations (event-related potentials (ERPs)) through sensor-wise neural activity estimation using local field potentials. ROI time-series were segmented into two-second epochs to capture attentional bias during death-related cue processing. Subject-level DCMs employed a frequency range of 1–40 Hz and a temporal window of 1–200 ms post-stimulus. The 200 ms window captures early attentional orienting processes, given that ERP research demonstrates that these early responses are critical for attention to emotional faces (Luo et al., 2010; Wessing et al., 2017), and MEG studies show similar patterns (Monroe et al., 2013; Peyk et al., 2008). This 200 ms window encompasses automatic attentional capture while potentially maximizing the detection of individual differences in oscillatory responses to death-related cues. Early MEG responses provide higher signal-to-noise ratios before movement artifacts and cognitive interference accumulate (Gross et al., 2013). The 1–40 Hz frequency range captures theta to low beta bands (3–20 Hz) associated with attentional encoding and memory formation in the subsequent recognition task (Ostrowski and Rose, 2024), extended to include early gamma frequencies for comprehensive attentional allocation and memory process.

The DCM model parameters were then optimized to reproduce the observed neural dynamics in the key ROIs (VC, SPL, EC, and MTG). Though bilateral response to the task was observed, brain activity was modeled in the left hemisphere for DCM analyses. This decision was made: (1) to reduce computational load; (2) because this was a verbal task with mortality cues, likely involving impaired connectivity in the Broca's area (Costanza et al., 2021); and (3) because most participants were right-handed. One review paper suggested hemisphere-specific functions in emotional word processing based on time course: left hemisphere for fast, automatic processes and right hemisphere for slow, executive, and memory processes (Abbassi et al., 2011). This suggests that the left hemisphere is useful for capturing automatic neural functions relevant to acute attentional bias. Although the right hemisphere also plays a critical role in visuospatial attention (de Schotten et al., 2011) and may be relevant to attentional bias, it was not examined in the current study.

After individual DCM estimation, predicted and observed evoked responses were compared for similarity. Individual DCMs showing fit indices greater than two standard deviations below the median between evoked and modeled responses were retained for subsequent analyses. The threshold was selected to ensure model accuracy by quantifying explained variance, confirming reliable representation of underlying data. Among 53 participants (Fig. 1), five individual DCMs were excluded due to non-convergence from poor MEG data quality (2 SR, 2 CC, 1 HV), with no group differences in exclusion rates ($\chi^2(2) = 0.60$, $p = .740$). Two additional SR participants were excluded for poor model accuracy, yielding no significant group difference in overall exclusions ($\chi^2(2) = 4.59$, $p = .101$). Furthermore, Kruskal–Wallis rank sum test results showed that correlations between predicted and observed event-related potentials did not differ across groups: SR (mean = 0.90, SD = 0.09), CC (mean = 0.92, SD = 0.08), and HV (mean = 0.91, SD = 0.08). These exclusions resulted in 46 participants for group-level DCM analysis. Individual DCMs underwent group-level Bayesian model comparison using parametric empirical Bayes (PEB) estimation (Zeidman et al., 2019), providing robust statistical inference about group differences in underlying generative mechanisms. Three general linear models (GLMs) were constructed for group comparisons in second-level design analysis. Within each model, the first column tested the grand mean across all participants (column of ones), while the third and fourth columns included covariates for scaled age and biological sex, respectively. The second column tested group differences: model one compared the SR (1) and CC (0) groups, model two compared the SR (1) and HV (0) groups, and model three compared the CC (1) and HV (0) groups.

2.6. Data analysis plan

Statistical analyses were conducted to compare the demographic and clinical characteristics, as well as the reaction times, of the SR, CC, and HV groups. Analysis of variance (ANOVA) and chi-squared tests were used to evaluate demographic differences between the groups, with age, biological sex, and ethnicity entered as covariates. The extent of missing

data for reaction times was assessed to ensure that data quality did not impact the observed differences in reaction times among the groups. Differences in anxiety and depressive symptoms were analyzed using one-way ANOVA, with depressive (MADRS and HAMD-24) and anxiety symptom (HAM-A) scores entered as dependent variables. The group was entered as the independent variable, while age and biological sex were included as covariates. A linear mixed model (3dLMEr) in AFNI was used to identify potential brain regions (i.e., clusters) showing group differences in MEG signals (SR vs. HV; SR vs. CC), with age and session as covariates. To estimate omission and commission error rate differences, a binomial GLM was conducted, and the interaction effects of condition (DC (death congruent), DI (death incongruent), LC (life congruent), LI (life incongruent), NN (neutral); reference: NN) and group (SR, CC, and HV) were estimated. Scaled age and biological sex (female as reference) were included as covariates.

The main effects were mean differences between groups, regardless of group membership. Interaction effects assessed the relationship between group membership and task conditions. Task conditions were categorized by collapsing relevant trial types in the life/death dot-probe task: for example, the death condition was defined by combining death-congruent and death-incongruent trials to enhance statistical power and interpretability. Significant brain clusters were determined using cluster-based multiple comparison correction (3dClustSim) with family-wise error (FWE) correction. To provide a fuller spectrum of results, findings from liberal ($p < .08$, FWE-corrected) to stringent ($p < .001$, FWE-corrected) significance thresholds are reported. Cluster-wise averaged effect sizes were reported for the early VC, SPL, EC, and MTG.

The DCM model for sensory information processing regions was developed based on the group analysis results. For each individual, three variations of the DCM model were estimated, modifying the proposed effective connectivity between the specified brain regions using B matrices. The design matrix discriminated the main effects of each condition (death, life, congruent, and incongruent) while collapsing relevant trials (Figs. 3 and 4). Model 1 included fully reciprocated feedforward and feedback connections between the early VC, SPL, EC, and MTG. This architecture was based on established functional roles: the VC transmits visual information to higher-order regions; the SPL integrates visuospatial information and directs spatial attention (Culham and Kanwisher, 2001); the EC receives sensory inputs from insular and piriform cortices and projects to basal ganglia and parahippocampal regions, supporting visuospatial processing, episodic memory, and contextual updating (Aminoff et al., 2013; Kerr et al., 2007); and the MTG contributes to semantic memory processing within the posterior heteromodal association cortex, particularly for social cognition, theory of mind, and semantic decision-making (Binder et al., 2009; Schurz et al., 2014). In Model 2, the VC carried feedforward signals to the SPL, EC, and MTG, whereas the SPL carried feedforward signals to the EC and MTG. The EC also carried the feedforward signal to the MTG. This model tested the hypothesis of unidirectional information flow with progressive visual processing from low- to high-order regions. The model assumed visual information would be updating, but not reciprocally. In Model 3, the VC carried feedforward signals to the SPL, EC, and MTG directly. This model assumed independent processing of visual information across regions without active inter-regional linking. The estimated negative free energy bound of the log-model evidence score of each model, which suggests the relative explained variance, was compared using the fixed-effect analysis of the Bayesian model. The model with the highest log-model evidence score (Model 1) was then selected for subsequent analyses (Fig. 5).

Finally, PEB analysis was applied to explore group differences in connectivity between the specified brain regions. The study focused on feedforward and feedback connectivity. This model tested for group differences between the SR and HV, SR and CC, and CC and HV groups. Parameters with a posterior probability (posteriorp) of >0.90 were considered significant, with a free energy approach to account for covariance among parameters and covariates. Age and biological sex were included as covariates due to their associations with brain volume in individuals with a history of suicide attempts (Gifuni et al., 2021). To assess whether task conditions affected efferent connectivity in the specified brain regions beyond the main effect of group differences, the main effect of task conditions (death, life, congruent, and incongruent) on connectivity was assessed while controlling for group differences, age, and biological sex. The design matrix included four parameters in each column, including intercept, group differences, age, and biological sex, allowing for modulations on all connections within each condition, and each condition was specified using a B Matrix.

3. Results

3.1. Descriptive statistics and clinical scales

There was no difference between the groups in terms of biological sex or race. Group differences emerged for age ($F(2, 50) = 8.88$, $p < .001$, $\eta 2 = 0.26$), with individuals in the HV group being younger than those in the CC group (Mdiff = −16.44, $p < .001$). The SR group did not differ from the CC (Mdiff = -9.32, $p = .061$) or HV group (Mdiff = 7.12, $p = .172$). Significant group differences were also observed in severity of depressive symptoms, as measured by the MADRS and HAMD-24, as well as the severity of anxiety symptoms, as assessed by the HAM-A (see Table 1). Scores for these measures were comparable between individuals in the SR and CC groups, both of whom had higher scores than the HV group. To assess face validity, group differences in suicide risk, as

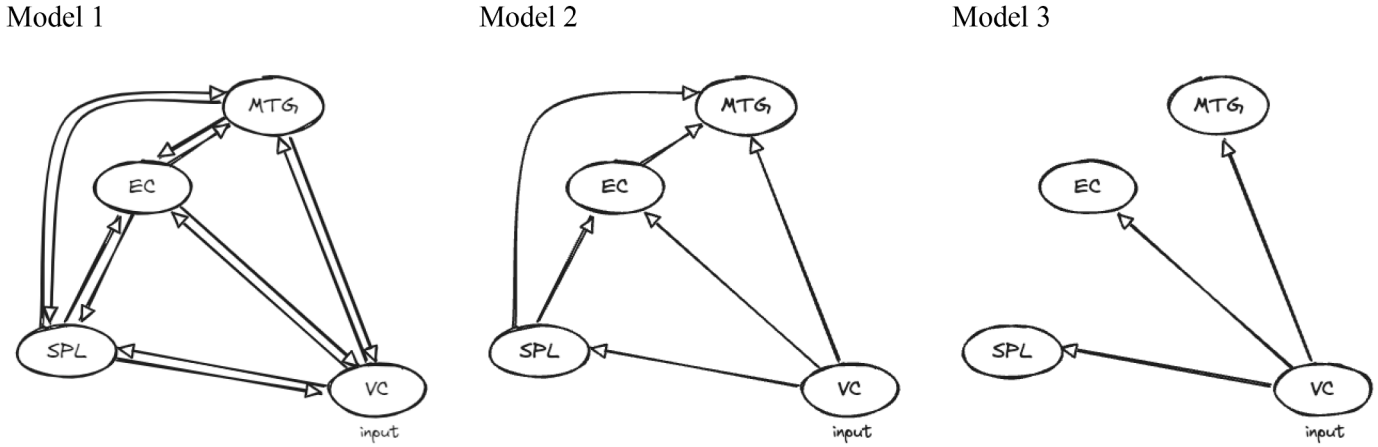

Fig. 3. Establishing effective connectivity using Dynamic Causal Modeling (DCM) across three potential models. EC: early visual cortex; SPL: superior parietal lobule; EC: entorhinal cortex; MTG: middle temporal gyrus.

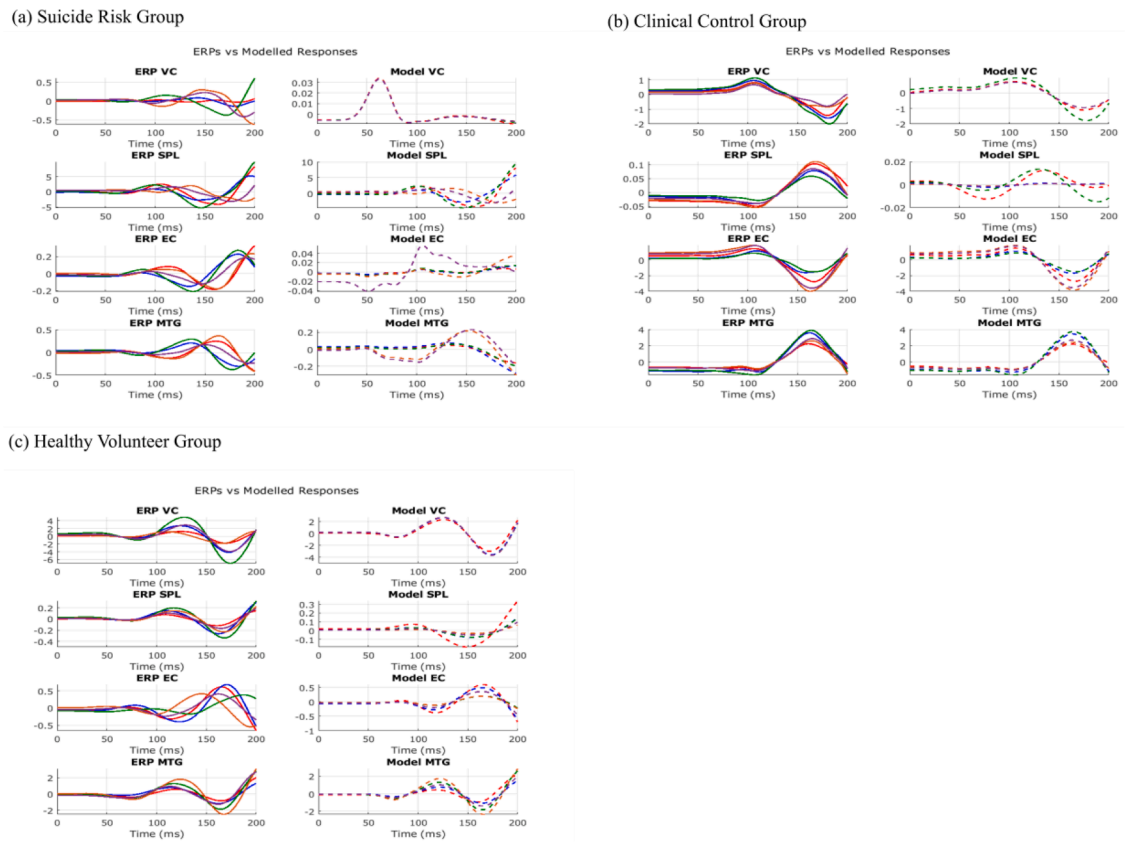

Fig. 4. Individual dynamic causal modeling (DCM) estimation across groups and conditions: DC (death congruent; red), DI (death incongruent; blue), LC (life congruent; green), LI (life incongruent; orange), and NN (neutral; purple). VC: primary visual cortex; SPL: superior parietal lobule; EC: entorhinal cortex; MTG: middle temporal gyrus; ERP: event-related potential.

measured by the SSI, were explored. Although current suicide ideation did not significantly differentiate between the SR and CC groups ($F(2, 36) = 2.71$, $p = .080$, $\eta 2 = 0.12$), past suicide ideation did ($F(2, 29) = 11.80$, $p < .001$, $\eta 2 = 0.43$). Individuals in the SR group had a higher frequency of past suicide ideation than those in the CC (Mdiff = 13.57, $p < .001$) or HV (Mdiff = 25.88, $p = .023$) groups.

3.2. Behavioral analysis in the life/death dot-probe task

Reaction time was calculated only for correct trials. The number of missed trials did not differ between the groups (F (2, 44) = 1.61, $p = .211$, $\eta 2 = 0.09$). Reaction time in the different conditions was examined to compare behavioral outcomes between groups on the life/death dot-probe task. No difference was observed between the groups for any of the conditions: ($F(2, 43) = 0.32$, $p = .731$, $\eta 2 = 0.04$ for death congruent; $F(2, 43) = 0.50$, $p = .809$, $\eta 2 = 0.05$ for death incongruent; $F(2, 43) = 0.32$, $p = .728$, $\eta 2 = 0.04$ for life congruent; and $F(2, 43) = 0.20$, $p = .816$, $\eta 2 = 0.04$ for life incongruent conditions, respectively). Commission errors for neutral conditions were omitted due to the recording issue, so the reference group of analysis was the LC group (see Tables 2 and 3). No group or condition differences were noted for commission rates (ps > 0.05), and post-hoc analyses confirmed no group differences (ps $\geq .05$). With regard to omission rates, the SR group showed zero omissions across all trials except one DC trial, leading to complete separation and non-identifiable logistic regression coefficients. Thus, per-subject omission proportions were aggregated and fit to a linear mixed model; no group or condition differences in omission rates were observed (ps > 0.05).

3.3. Group differences in oscillating MEG power during the life/death dot-probe task

Source-localized power in the theta, alpha, beta, and gamma bands was analyzed using linear mixed models ($n = 53$). The model examined significant clusters showing group differences (SR, CC, and HV) while controlling for age and biological sex (see Table 4 and Fig. 6). These regions included the superior/inferior frontal gyrus, inferior temporal gyrus, inferior parietal lobule, superior occipital gyrus, MTG, middle orbital gyrus, supplementary motor area, precentral/postcentral gyrus, SPL, cuneus, EC (adjacent to the parahippocampal gyrus), precuneus, and cerebellum across multiple bands. Among the brain clusters showing reduced activity in the SR group compared to the other groups, four key brain regions potentially related to sensory processing and attentional bias were selected: the early VC, SPL, EC, and MTG. When collapsing across all conditions, individuals in the SR group had significantly reduced MEG power in these brain regions compared to the CC and HV groups, except for the SPL (see Table 5). This pattern was particularly noticeable for the death and incongruent conditions.

3.4. Dynamic causal modeling

The DCM model investigated effective connectivity among four key brain regions potentially related to sensory processing and attentional bias: the early VC, SPL, EC, and MTG. As noted above, among three possible model architectures, Model 1 provided the best fit, including fully reciprocated feedforward and feedback connections between these regions ($posteriorp = 1$; Fig. 5). Age and biological sex were included as covariates in the model estimation. During the inversion, significant levels of DCM connectivity were estimated using the variational free energy method, with a posterior probability > 0.9.

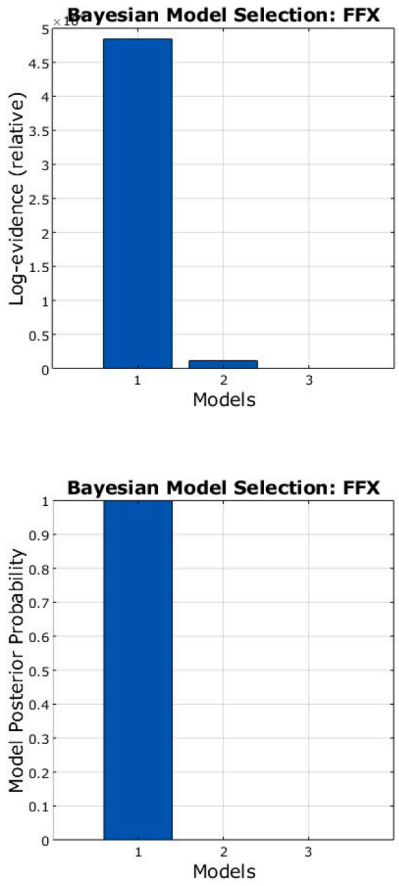

Fig. 5. Comparison of the three potential models using the fixed-effect analysis of the Bayesian model selection. The most successful model (Model 1) showed the highest fixed effects based on the log-model evidence score and was selected for subsequent analyses.

Compared to the CC and HV groups, individuals in the SR group showed decreased feedforward connectivity from the VC to the SPL, EC, and MTG, and decreased bidirectional signaling between the MTG and SPL across all conditions (*posteriorp* = 1; see Table 6 and Fig. 7). The SR group also showed increased feedforward connectivity from the SPL to the EC and heightened feedback connectivity from the MTG to the VC (*posteriorp* = 1). These results suggest that individuals in the SR group may struggle with sensory information processing and integration while still attempting to update contextual information from the SPL to the EC.

In the death condition, which was created by collapsing the death congruent and death incongruent conditions, the SR group showed decreased connectivity from the VC to the EC and MTG and from the SPL to the MTG, compared to the CC and HV groups (*posteriorp* = 1). The SR group also showed decreased connectivity from the EC to the SPL (*posteriorp* = 1). In the life condition, created by collapsing the life congruent and life incongruent conditions, the SR group showed decreased connectivity from the MTG to the SP (*posteriorp* = 1). In the congruent condition, created by collapsing the death congruent and life congruent conditions, the SR group showed an increased constraint on bottom-up sensory processing from the EC to the MTG, with decreased connectivity between the SPL and MTG compared to the CC and HV groups (*posteriorp* = 1). In the incongruent condition, created by collapsing the death incongruent and life incongruent conditions, the SR group displayed reduced connectivity from the VC to the MTG and from the EC to the SP (*posteriorp* = 1).

As an exploratory analysis, DCM analysis was conducted with primary diagnosis as a covariate because a trend-level group difference for primary diagnosis was noted between the SR and CC groups ($\chi^2(1) = 3.54$, $p = .060$) that may potentially have contributed to the DCM results. Compared to the results seen in Table 3, the DCM results that included the primary diagnosis covariate maintained all associations in the same direction and at similar strengths (see Table 7), suggesting that primary diagnosis did not substantially contribute to the DCM results.

4. Discussion

This study used the life/death dot-probe task to investigate attentional bias as a potential neurobiological marker of suicide risk and is the

Table 3
Commission error rate comparisons among conditions.

Comparison groups		Condition			Condition: SR		
Target	Reference	Effects	SE	*p*-value	Effects	SE	*p*-value
LC	DC	-0.66	0.42	.231	0.23	0.36	.638
LC	DI	-0.73	0.43	.231	-0.44	0.36	.565
LC	LI	-0.85	0.42	.231	-0.16	0.36	.655
DC	DI	-0.07	0.29	.811	-0.67	0.36	.386
DC	LI	-0.19	0.27	.740	-0.39	0.36	.565
DI	LI	-0.12	0.29	.811	0.28	0.35	.638

DC: death coherent; DI: death incoherent; LC: life coherent; LI: life incoherent.

Table 2
Commission and omission error rates among different conditions and groups.

	Commission error				Omission error			
	Effects	SE	*z*-score	*p*-value	Effects	SE	*t*-value	*p*-value
Intercept	-0.72	1.20	-6.05	<0.001	0.02	0.02	1.31	.198
DC	1.79	1.09	1.64	.100	0.002	0.006	0.33	.745
DI	1.61	1.10	1.46	.144	-0.0003	0.006	-0.04	.966
LC					0.001	0.006	0.17	.863
LI	2.09	1.07	1.96	.050	-0.001	0.006	-0.21	.832
SR	2.69	1.37	1.96	.050	-0.01	0.02	-0.49	.628
CC	0.75	1.38	0.54	.589	-0.01	0.02	-0.48	.633
Age	0.20	0.41	0.48	.630	0.02	0.009	1.99	.054
Sex (M)	-0.89	0.71	-1.25	.211	-0.004	0.02	-0.24	.813
DC:SR	-2.02	1.15	-1.76	.078	0.0006	0.01	0.05	.958
DI:SR	-1.17	1.16	-1.01	.312	0.0003	0.01	0.02	.981
LC:SR					-0.001	0.01	-0.10	.924
LI:SR	-1.93	1.13	-1.72	.086	0.001	0.01	0.12	.907
DC:CC	-1.37	1.21	-1.13	.259	0.01	0.007	1.37	.173
DI:CC	-1.46	1.24	-1.18	.239	-0.004	0.007	-0.52	.605
LC:CC					0.002	0.007	0.30	.764
LI:CC	-1.80	1.20	1.50	.134	-0.003	0.007	-0.39	.700

DC: death coherent; DI: death incoherent; LC: life coherent; LI: life incoherent; SR: suicide risk group; CC: clinical controls group.

Table 4
Significant clusters showing group differences in magnetoencephalography (MEG) power using Analysis of Functional Neuroimages (AFNI).

Conditions	Target Group	Reference Group	Bandwidths	Hemisphere	ROIs	*p*-value (FWE-corrected)	Voxels	Coordinates		
								x	y	z
Averaged over conditions	SR	CC	alpha	right	middle temporal gyrus	<0.01	1818	-62	42	2
	SR	CC	alpha	left	middle temporal gyrus	<0.01	1786	60	14	-16
	SR	CC	beta	left	entorhinal cortex	<0.05	1083	30	14	-30
	SR	CC	gamma	left	entorhinal cortex	<0.08	752	28	14	-30
	SR	HV	theta	left	cuneus	<0.01	1645	6	82	32
	SR	HV	theta	right	postcentral gyrus	<0.01	1550	-44	22	38
	SR	HV	alpha	right	superior parietal lobule	<0.05	950	-18	54	62
	SR	HV	beta	left	cuneus	<0.01	2123	6	86	34
	SR	HV	beta	right	middle temporal gyrus	<0.05	832	-52	62	14
	SR	HV	gamma	right	inferior frontal gyrus	<0.001	2536	-48	-16	30
	SR	HV	gamma	right	cuneus	<01	1639	-10	82	38
	SR	HV	gamma	left	cerebellum	<0.01	1436	24	92	-20
	SR	HV	gamma	left	superior occipital gyrus	<0.01	1396	18	82	38
	SR	HV	gamma	right	postcentral gyrus	<0.01	1280	-44	22	38
	SR	HV	gamma	left	postcentral gyrus	<0.05	967	6	12	66
	SR	HV	gamma	right	postcentral gyrus	<0.05	872	44	-22	28
Death	SR	CC	alpha	left	middle temporal gyrus	<0.01	1499	56	16	-16
	SR	CC	alpha	left	inferior frontal gyrus	<0.01	1424	22	-26	-18
	SR	CC	alpha	left	middle orbital gyrus	<0.05	1028	6	-54	-10
	SR	CC	beta	left	entorhinal cortex	<0.001	2556	28	14	-30
	SR	CC	gamma	left	entorhinal cortex	<0.05	1016	26	14	-30
	SR	HV	theta	left	inferior frontal gyrus	<0.001	2248	42	24	38
	SR	HV	theta	right	inferior frontal gyrus	<0.01	1708	-42	24	40
	SR	HV	theta	left	cuneus	<0.01	1529	6	82	32
	SR	HV	alpha	left	cuneus	<0.01	1363	2	82	8
	SR	HV	alpha	right	superior parietal lobule	<0.05	959	-18	54	62
	SR	HV	alpha	left	middle orbital gyrus	<0.05	887	34	-40	-14
	SR	HV	beta	left	cuneus	<0.001	3230	6	86	34
	SR	HV	beta	left	middle frontal gyrus	<0.05	981	44	-38	14
	SR	HV	gamma	left	cerebellum	<0.001	3746	24	92	-20
	SR	HV	gamma	right	middle frontal gyrus	<0.001	2746	-28	-28	38
	SR	HV	gamma	right	postcentral gyrus	<0.01	1726	-44	22	38
	SR	HV	gamma	left	cuneus	<0.01	1462	10	82	38
	SR	HV	gamma	left	superior frontal gyrus	<0.01	1444	6	12	68
	SR	HV	gamma	left	superior occipital gyrus	<0.01	1273	18	82	38
	SR	HV	gamma	left	inferior parietal lobule	<0.01	1129	42	24	34
	SR	HV	gamma	left	inferior frontal gyrus	<0.05	1090	48	-20	30
Life	SR	CC	theta	right	precuneus	<0.001	2609	-8	38	68
	SR	CC	theta	right	superior occipital gyrus	<0.01	1179	-26	62	42
	SR	CC	alpha	left	postcentral gyrus	<0.001	9204	50	18	50
	SR	CC	alpha	left	middle temporal gyrus	<0.001	2237	60	14	-16
	SR	CC	alpha	left	inferior frontal gyrus	<0.01	2068	40	-32	-16
	SR	CC	alpha	right	superior parietal lobule	<0.05	913	-32	64	54
	SR	CC	beta	left	precentral gyrus	<0.01	1419	22	10	70
	SR	CC	beta	left	middle temporal gyrus	<0.01	1290	60	14	-16
	SR	CC	beta	left	entorhinal cortex	<0.05	867	30	10	-32
	SR	CC	gamma	left	precentral gyrus	<0.001	2775	18	14	70
	SR	HV	theta	right	paracentral gyrus	<0.01	1387	-8	34	70
	SR	HV	theta	right	postcentral gyrus	<0.01	1357	-44	22	38
	SR	HV	theta	right	middle temporal gyrus	<0.05	864	-26	0	-44
	SR	HV	theta	left	middle temporal gyrus	<0.05	857	30	-14	-36
	SR	HV	alpha	left	precentral gyrus	<0.001	4507	20	10	70
	SR	HV	alpha	left	cerebellum	<0.01	2057	10	86	-10
	SR	HV	alpha	left	primary visual cortex	<0.05	939	10	84	40
	SR	HV	beta	left	cuneus	<0.001	5036	6	86	34
	SR	HV	beta	right	inferior temporal gyrus	<0.05	1039	-48	8	-40
	SR	HV	gamma	right	inferior frontal gyrus	<0.001	4519	-48	-16	30
	SR	HV	gamma	left	inferior frontal gyrus	<0.01	2246	46	-8	4
	SR	HV	gamma	right	superior occipital gyrus	<0.01	2195	-20	82	30
	SR	HV	gamma	left	cerebellum	<0.01	1962	24	92	-20
	SR	HV	gamma	left	superior occipital gyrus	<0.01	1648	20	80	34
	SR	HV	gamma	right	postcentral gyrus	<0.01	1326	-40	36	60
	SR	HV	gamma	right	entorhinal cortex	<0.05	908	-32	24	-24
Congruent	SR	CC	theta	left	precentral gyrus	<0.001	2181	20	14	70
	SR	CC	alpha	left	postcentral gyrus	<0.001	8709	32	30	62
	SR	CC	alpha	left	inferior frontal gyrus	<0.001	4344	40	-34	-16
	SR	CC	alpha	right	inferior temporal gyrus	<0.05	1038	-46	10	-40
	SR	CC	alpha	right	superior parietal lobule	<0.05	828	-32	64	54
	SR	CC	beta	left	postcentral gyrus	<0.01	2129	32	36	62
	SR	CC	beta	left	entorhinal cortex	<0.05	956	30	10	-32
	SR	CC	gamma	left	cerebellum	<0.001	3398	14	94	-18
	SR	CC	gamma	right	superior frontal gyrus	<0.01	1616	-22	14	66
	SR	CC	gamma	right	inferior occipital gyrus	<0.05	923	-36	90	-10

(*continued on next page*)

Table 4 (*continued*)

Conditions	Target Group	Reference Group	Bandwidths	Hemisphere	ROIs	*p*-value (FWE-corrected)	Voxels	Coordinates		
								x	y	z
	SR	HV	theta	right	middle orbital gyrus	<0.01	2022	-10	-48	-10
	SR	HV	theta	left	cuneus	<0.01	2017	6	82	32
	SR	HV	theta	right	postcentral gyrus	<0.01	1271	-44	22	38
	SR	HV	alpha	right	entorhinal cortex	<0.001	2761	-26	8	-32
	SR	HV	alpha	right	middle frontal gyrus	<0.001	2419	-28	-18	38
	SR	HV	alpha	right	middle orbital gyrus	<0.01	1997	-30	-40	-14
	SR	HV	alpha	left	inferior frontal gyrus	<0.01	1539	40	-34	-16
	SR	HV	alpha	left	entorhinal cortex	<0.01	1408	28	14	-30
	SR	HV	alpha	left	postcentral gyrus	<0.05	833	32	30	62
	SR	HV	beta	left	cuneus	<0.001	3139	6	86	34
	SR	HV	beta	right	middle temporal gyrus	<0.01	1317	-52	62	14
	SR	HV	beta	right	entorhinal cortex	<0.01	1116	-34	22	-26
	SR	HV	gamma	left	cerebellum	<0.01	5281	24	92	-20
	SR	HV	gamma	right	inferior frontal gyrus	<0.001	2488	-48	-16	30
	SR	HV	gamma	right	cuneus	<0.001	1644	-10	82	38
	SR	HV	gamma	right	postcentral gyrus	<0.01	1362	-44	22	38
	SR	HV	gamma	right	inferior temporal gyrus	<0.01	1327	-36	2	-40
	SR	HV	gamma	left	superior occipital gyrus	<0.01	1263	18	82	38
	SR	HV	gamma	left	supplementary motor area	<0.01	1179	8	8	68
	SR	HV	gamma	left	inferior frontal gyrus	<0.05	1048	44	-22	28
	SR	HV	gamma	left	inferior parietal lobule	<0.05	860	42	24	34
In-congruent	SR	CC	theta	right	superior temporal gyrus	<0.01	1356	-40	20	0
	SR	CC	theta	left	superior temporal gyrus	<0.01	1258	44	20	-2
	SR	CC	theta	right	cerebellum	<0.05	1036	-52	44	-26
	SR	CC	theta	left	superior frontal gyrus	<0.05	937	24	-58	14
	SR	CC	theta	right	superior frontal gyrus	<0.05	888	-24	-60	10
	SR	CC	alpha	left	middle temporal gyrus	<0.001	2614	60	14	-16
	SR	CC	alpha	left	middle orbital gyrus	<0.01	1089	6	-54	-10
	SR	CC	beta	left	entorhinal cortex	<0.001	2719	30	14	-30
	SR	CC	gamma	left	entorhinal cortex	<0.01	1201	28	14	-30
	SR	HV	theta	right	postcentral gyrus	<0.001	2339	-42	24	40
	SR	HV	theta	left	postcentral gyrus	<0.01	1418	42	24	38
	SR	HV	alpha	right	superior parietal lobule	<0.01	1238	-18	54	62
	SR	HV	beta	left	superior occipital gyrus	<0.001	3116	6	86	34
	SR	HV	beta	right	middle temporal gyrus	<0.05	853	-52	62	14
	SR	HV	gamma	right	middle temporal gyrus	<0.001	3457	-44	-38	16
	SR	HV	gamma	left	inferior frontal gyrus	<0.001	2587	46	-28	-2
	SR	HV	gamma	right	supplementary motor area	<0.001	2502	-6	18	66
	SR	HV	gamma	right	superior occipital gyrus	<0.01	2195	-20	82	30
	SR	HV	gamma	left	middle occipital gyrus	<0.01	1600	20	80	34
	SR	HV	gamma	left	inferior parietal lobule	<0.01	1222	42	24	38
	SR	HV	gamma	left	superior frontal gyrus	<0.05	971	6	12	66

The table displays source-based MEG clusters showing group differences across various bandwidths—including theta (4–8 Hz), alpha (9–14 Hz), beta (15–29 Hz), and gamma (30–58 Hz)—among the suicide risk group (SR), clinical controls (CC), and healthy volunteers (HV). The differences between the SR group and the two other groups (CC and HV) are reported. The differences are shown across different conditions: death, life, congruent, incongruent, and averaged over all conditions. FWE: family-wise error.

first MEG study to apply DCM to a life/death dot-probe task in a population at risk for suicide. The SR group showed increased source-level MEG power in response to the death and incongruent conditions but decreased power for life and congruent conditions across various brain regions. These regions included the frontal gyrus, inferior temporal gyrus, inferior parietal lobule, superior occipital gyrus, MTG, middle orbital gyrus, supplementary motor area, precentral/postcentral gyrus, cuneus, EC (adjacent to the parahippocampal gyrus), precuneus, and cerebellum across multiple bands. Collectively, these findings support our hypothesis and suggest impaired sensory information integration in individuals at risk for suicide. In addition, the DCM findings underscore that the SR group had less effective information transfer from the early VC to the EC and MTG and from the SPL to the MTG as well as diminished top-down regulatory signaling from the EC to the SPL in processing death-related cues. When participants were asked to allocate their attention to death/life-related words compared to neutral words, the MTG exerted a constraining influence on the EC through top-down signal processing. In contrast, when participants were asked to allocate their attention to neutral words compared to death/life-related words, there was less constraint in the reduced top-down signaling between the EC and the SPL.

Visual signal updating without sufficient sensory processing and integration may be a marker of suicide risk. Compared to the CC and HV groups, the SR group had significantly reduced feedforward signaling across multiple nodes of the visual processing hierarchy, specifically from the VC to the SPL, EC, and MTG, especially in response to death-related words. This suggests impaired sensory input updating to stimuli in individuals at risk for suicide. Increased feedforward signaling from the SPL to the EC was also observed in this group, which may indicate maladaptive hyperactivity or inefficient processing of external cues, regardless of death-related information loading. This finding aligns with the roles of the SPL and EC in visuospatial information processing and contextual updating (Culham and Kanwisher, 2001; Kerr et al., 2007; Aminoff et al., 2013). The SR group also showed increased feedback signaling from the MTG to the VC, which may indicate the system's attempt to prioritize salient information by filtering external cues through high-order regions (the MTG), potentially disrupting precise, non-salient semantic memory processing (Schurz et al., 2014). However, it may also suggest impaired 'bottom-up' processing, as indicated by reduced feedforward signaling from the VC to the MTG followed by increased 'top-down' signal information loading, as measured by increased feedback signaling from these regions as a compensatory mechanism. Future longitudinal research studies are needed to observe the communication from the VC to the MTG over time during the task.

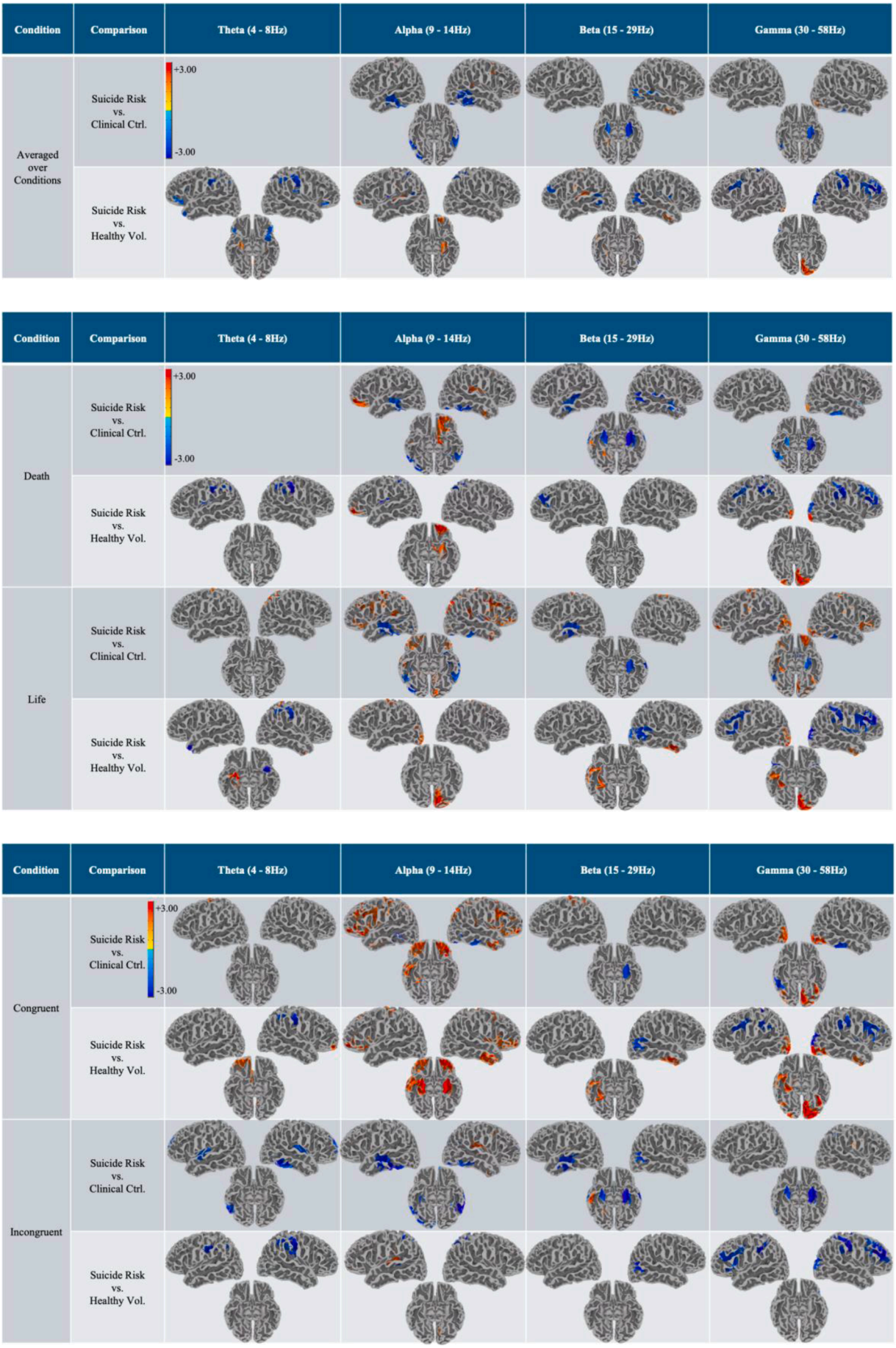

(caption on next page)

Fig. 6. The cross-condition and condition-specific band-limited power of the magnetoencephalography (MEG) signals in individuals in the suicide risk (SR) group. The figure illustrates source-based MEG power group differences across various bandwidths—including theta (4–8 Hz), alpha (9–14 Hz), beta (15–29 Hz), and gamma (30–58 Hz)—between the suicide risk group, clinical controls, and healthy volunteers. The differences are shown across different conditions: death, life, congruent, incongruent, and averaged over all conditions.

Table 5
Cluster-wise averaged effect sizes showing group differences in magnetoencephalography (MEG) power using Analysis of Functional Neuroimages (AFNI).

Conditions	Target group	Reference group	Bandwidths	Hemisphere	ROIs	Effect Size	Coordinates		
							x	y	z
Averaged over conditions	SR	CC	alpha	right	middle temporal gyrus	-2.24	-62	42	2
	SR	CC	alpha	left	middle temporal gyrus	-2.23	60	14	-16
	SR	CC	beta	left	entorhinal cortex	-2.51	30	14	-30
	SR	CC	gamma	left	entorhinal cortex	-2.26	28	14	-30
	SR	HV	alpha	right	superior parietal lobule	2.21	-18	54	62
	SR	HV	beta	right	middle temporal gyrus	-2.39	-52	62	14
Death	SR	CC	alpha	left	middle temporal gyrus	-2.21	56	16	-16
	SR	CC	beta	left	entorhinal cortex	-2.68	28	14	-30
	SR	CC	gamma	left	entorhinal cortex	-2.60	26	14	-30
	SR	HV	alpha	right	superior parietal lobule	-2.42	-18	54	62
Life	SR	CC	alpha	left	middle temporal gyrus	-2.34	60	14	-16
	SR	CC	alpha	right	superior parietal lobule	2.40	-32	64	54
	SR	CC	beta	left	middle temporal gyrus	-2.31	60	14	-16
	SR	CC	beta	left	entorhinal cortex	-2.34	30	10	-32
	SR	HV	theta	right	middle temporal gyrus	2.39	-26	0	-44
	SR	HV	theta	left	middle temporal gyrus	-2.89	30	-14	-36
	SR	HV	alpha	left	primary visual cortex	-2.24	10	84	40
	SR	HV	gamma	right	entorhinal cortex	2.17	-32	24	-24
Congruent	SR	CC	alpha	right	superior parietal lobule	2.26	-32	64	54
	SR	CC	beta	left	entorhinal cortex	-2.51	30	10	-32
	SR	HV	alpha	right	entorhinal cortex	2.46	-26	8	-32
	SR	HV	alpha	left	entorhinal cortex	2.81	28	14	-30
	SR	HV	beta	right	middle temporal gyrus	-2.25	-52	62	14
	SR	HV	beta	right	entorhinal cortex	2.25	-34	22	-26
In-congruent	SR	CC	alpha	left	middle temporal gyrus	-2.73	60	14	-16
	SR	CC	beta	left	entorhinal cortex	-2.61	30	14	-30
	SR	CC	gamma	left	entorhinal cortex	-2.87	28	14	-30
	SR	HV	alpha	right	superior parietal lobule	-2.42	-18	54	62
	SR	HV	beta	right	middle temporal gyrus	-2.57	-52	62	14
	SR	HV	gamma	right	middle temporal gyrus	-2.79	-44	-38	16

The table displays source-based MEG power group differences across various bandwidths—including theta (4–8 Hz), alpha (9–14 Hz), beta (15–29 Hz), and gamma (30–58 Hz)—among the suicide risk (SR), clinical control (CC), and healthy volunteer (HV) groups. The differences between the SR group and the two other groups (CC and HV) are reported. Differences are shown across different conditions: death, life, congruent, incongruent, and averaged over all conditions. FWE: family-wise error.

The SPL is known to play a role in attention orientation and in the control and maintenance of attention (Corbetta and Shulman, 2002; Schrooten et al., 2017), and it receives multimodal sensory inputs. It is part of the entorhinal-retrosplenial circuit and contributes to spatial sensory processing like physical navigation (Dutriaux et al., 2024); the SPL also functions within the dorsal visual stream, where it is involved in processing visual motion and actions in space (Rolls et al., 2023).

The EC functions as a relay station between the neocortex and hippocampus and facilitates memory and learning through synaptic plasticity, especially long-term potentiation (Yaniv et al., 2003). In addition, it integrates sensory information relevant to memory and navigation (Agster and Burwell, 2013; Grande et al., 2022). The EC projects to the amygdala, influencing connections between the amygdala and thalamic reticular nucleus, which impacts attentional processes (John et al., 2016; Zikopoulos and Barbas, 2012). The EC also receives integrated sensory inputs from the superior temporal gyrus (Amaral et al., 1983), suggesting that it may play a central role in coordinating sensory information with emotional and spatial memory.

Finally, the MTG helps integrate multimodal sensory information and is also associated with lexical-syntactic properties (Snijders et al., 2010). The MTG may act as a hub linking spatial information across regions, potentially including the SPL and EC, although the precise directional connections between these regions have yet to be explored.

Collectively, our findings suggest that disrupted visual signal updating across these regions—particularly in response to death-related cues—may reflect underlying vulnerability to suicide risk. Visual signal processing, particularly within this network, is still underexplored in the context of suicide. These findings further suggest that the MTG plays a critical role in signal processing and integration, particularly in the context of death-related and emotional attention orientation. Specifically, the MTG constrained visual signal sources originating from the VC and the SPL in response to death-related words but executed fewer constraints on visual signals from the SPL when processing life-related words. This pattern suggests that the MTG selectively regulates the integration of death-related cues while allowing more flexible processing of non-death-related cues. Furthermore, when participants directed their attention towards death- or life-related words compared to neutral words, the MTG exerted a top-down constraining influence on the EC. In contrast, when participants focused on neutral words rather than emotionally salient words, there was a reduction in top-down signaling between the EC and the SPL, indicating less constraint. Taken together, these findings suggest that the MTG modulates sensory integration when attention is allocated away from emotionally salient stimuli, such as death-related cues.

Supporting evidence from prior research similarly suggests that the MTG might be linked to suicide risk. For instance, one study found increased connectivity between the MTG and the default mode network in veterans with a history of suicide attempts (Jagger-Rickels et al., 2023). The methodological approach of this study, however, relied on bidirectional correlation, which differs from our approach, which applied a generative model within a Bayesian framework to estimate directional associations between ROIs, providing more specific insights

Table 6
Comparing dynamic causal modeling (DCM) connectivity between the groups in different conditions.

Conditions	To	Suicide Risk vs. Clinical Controls				Suicide Risk vs. Healthy Volunteers				Clinical Controls vs. Healthy Volunteers			
		VC	SPL	EC	MTG	VC	SPL	EC	MTG	VC	SPL	EC	MTG
Forward (SP to SS)	VC						0.206				-0.244		-0.270
	SPL	-0.384				-0.543							
	EC									-0.403	-0.206		-0.229
	MTG	-0.560				-0.626							
Forward (SP to DP)	VC												
	SPL	-0.186			-0.250	-0.334			-0.276				
	EC	-0.368	0.180			-0.422	0.250				0.242		0.277
	MTG	-0.406	-0.310			-0.453	-0.309				0.336		
Backward (DP to SP)	VC												
	SPL								0.219			0.217	
	EC												
	MTG	0.257				0.396				0.522			
Backward (DP to II)	VC											0.305	0.221
	SPL												
	EC									0.361			
	MTG	0.382				0.486				0.473			
Death	VC												-0.346
	SPL			-0.317				-0.526					
	EC	-0.384				-0.527							
	MTG	-0.381	-0.470			-0.562	-0.576			-0.763		-0.656	
Life	VC								-0.361				-0.579
	SPL				-0.379				-0.479	-0.506			
	EC												
	MTG										-0.445		
Congruent	VC								-0.344				-0.659
	SPL				-0.463				-0.650				
	EC				0.325				0.340				
	MTG		-0.429				-0.461			-0.685		-0.607	
Incongruent	VC										-0.315		
	SPL			-0.291				-0.380					-0.324
	EC												
	MTG	-0.468				-0.563					-0.415	-0.362	

DP: deep pyramidal cells; SP: superficial pyramidal cells; SS: spiny stellate cells; II: inhibitory interneurons; VC: early visual cortex; SPL: superior parietal lobule; EC: entorhinal cortex; MTG: middle temporal gyrus. The posterior probability of the reported connectivities was 1.

into the directionality of this connectivity. Additional validation of statistical approaches in this context may further clarify these findings. Furthermore, a meta-analysis identified a positive association between MTG activation and suicide thoughts in general (Chen et al., 2022), though the study's larger sample size introduced heterogeneity in participant backgrounds. Further validation with larger, homogeneous samples may help refine the reliability of our findings.

The results of the present study also identified increased sensory information updating from the SPL to the EC, particularly during death-related cue processing and incongruent conditions. The SPL is essential for attention orientation and is positively associated with visual and attention networks, as well as with the sensorimotor and salience networks, which contribute significantly to visual signaling integration (Alahmadi, 2021). The integrated sensory information is then projected to the EC, where it updates spatial and mnemonic interference (Reagh and Yassa, 2014) and subsequently supports spatial memory (Malone et al., 2023) and mental representation of the self (Meneghetti et al., 2014). However, continuous updating of spatial and mnemonic interference and self-representation without sufficient signal processing may be inefficient from a neural energy standpoint, potentially leading to rigid responses to environmental changes. The role of SPL- and EC-driven context updating warrants further exploration, particularly in death-related cue processing and under neutral conditions in individuals at risk for suicide.

It should be noted that no difference in reaction time was observed between the groups, echoing previous studies that similarly found no significant reaction time differences between individuals with and without suicide risk. For instance, two studies that used the suicide dot-probe task and the Suicide Stroop Task compared individuals with a history of suicide attempts to those with suicide ideation and found that neither factor was associated with attentional bias (Mandel et al., 2025; Rogers et al., 2023). Furthermore, although one meta-analysis found that individuals with a history of suicide attempts tended to show attentional bias towards suicide-related cues compared to clinical controls, the effect size was small (Richard-Devantoy et al., 2016). Taken together, the results suggest that reaction time is not likely to differentiate between varying degrees of suicide risk and control groups. This may be attributed to the poor test-retest reliability of these tasks or, in the case of our study, may simply reflect that the death/life dot-probe task lacks sufficient sensitivity to detect attentional biases towards death-related cues at the behavioral level. To address some of these potential issues, another study used ecological momentary assessment over several days to examine continuous measures of suicide ideation and attentional control via the continuous performance task and found no relationship between the variability or intensity of attentional control and suicide ideation (Herzog et al., 2023). Although the death/life dot-probe task may not effectively capture behavioral differences across degrees of suicide risk, our findings indicate that suicide risk contributes to source-estimated power and effective connectivity among sensory processing brain regions, underscoring the potential value of suicide-related stimuli in identifying neural markers of suicide risk. Importantly, our neural findings are not confounded by behavioral differences, highlighting the task's unique ability to detect suicide risk.

The lack of behavioral differences between the groups may stem from the distinction between sensory processing and attentional and behavioral manifestations. Our findings suggest that cognitive activities in brain regions related to signal processing and integration might not initially manifest as attentional orientation and behavior. According to the information processing theory (Atkinson, 1968), this process can be categorized as sensory memory, which occurs before attention is

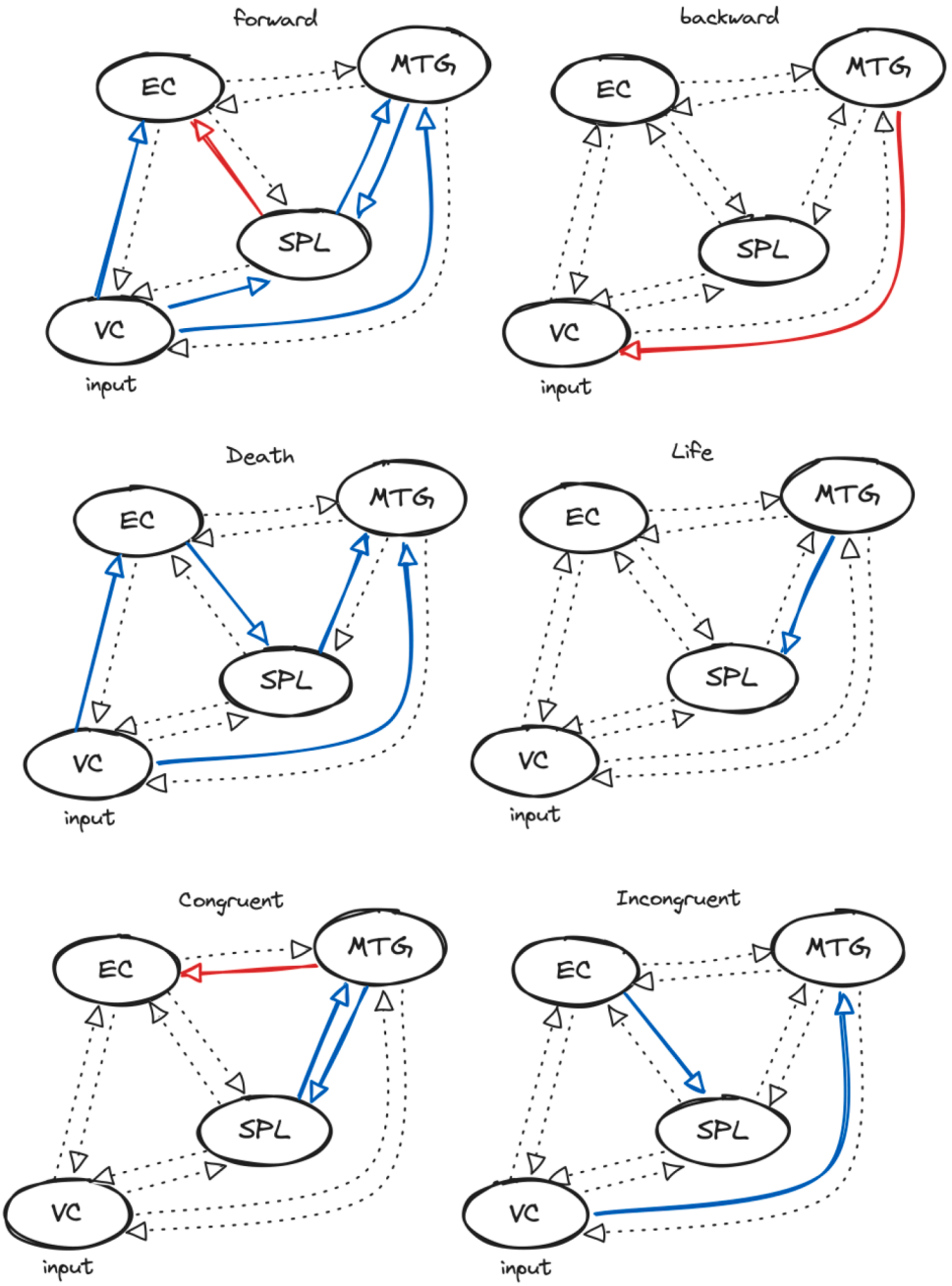

Fig. 7. Dynamic causal modeling (DCM) of effective connectivity in the suicide risk (SR) group compared to the other groups. The figure illustrates positive (red) and negative (blue) effective connectivities between brain regions, including the early visual cortex (VC), superior parietal lobule (SPL), entorhinal cortex (EC), and middle temporal gyrus (MTG).

allocated, making it less likely to influence behavior. While extensive research has focused on how attention refines sensory information and influences behavior (Correa et al., 2005; Gutnisky et al., 2009; Murai and Whitney, 2021), the role of sensory memory in suicide is less well understood. Some studies suggest that those who attempt suicide display increased tolerance for aversive sensations, including social pain, linked to reduced insula activity and inefficient sensory processing (DeVille et al., 2020; Risch et al., 2023). Our findings support the notion that inefficient sensory processing may contribute to suicide risk, although the relationship between sensory sensitivity and suicide risk is complex and not straightforward (Smith et al., 2021). Further research is needed to understand how altered sensory processing impacts cognitive and behavioral outcomes in individuals at risk for suicide.

Computational modeling offers a promising approach to better understand the relationship between ongoing sensory processing and suicide risk. While reinforcement learning models have been used to explore suicide risk, they often lack sensory-level inputs (Dixon-Gordon et al., 2022; Dombrovski and Hallquist, 2017; Dombrovski et al., 2019). In contrast, the dynamic interoceptive learning model provides a theoretical foundation for integrating sensory processing into computational models (Petzschner et al., 2021, 2017; Seth and Friston, 2016; Stephan et al., 2016; Toussaint et al., 2024). Future research could measure attentional biases and valence-dependent decision-making in individuals with suicide risk, while also accounting for their interoceptive and nociceptive sensitivity. Introducing multimodal sensory stimuli, such as auditory and tactile stimuli, as well as sensory-oriented emotional stimuli, may clarify how sensory processing influences attentional dynamics and decision-making in this population. This

Table 7
Comparing dynamic causal modeling (DCM) connectivity between the suicide risk (SR) and clinical control (CC) groups with primary diagnosis as a covariate.

Conditions	To	With primary diagnosis			
		VC	SPL	EC	MTG
Forward (SP to SS)	VC				
	SPL	-0.400			
	EC				
	MTG	-0.589			
Forward (SP to DP)	VC				
	SPL	-0.187			-0.229
	EC	-0.311	0.187		
	MTG	-0.409	-0.311		
Backward (DP to SP)	VC				
	SPL				
	EC				
	MTG	0.203			
Backward (DP to II)	VC				
	SPL				
	EC				
	MTG	0.336			
Death	VC				
	SPL			-0.369	
	EC	-0.377			
	MTG	-0.388	-0.523		
Life	VC				
	SPL				-0.400
	EC				
	MTG				
Congruent	VC				
	SPL				-0.527
	EC				0.307
	MTG		-0.422		
Incongruent	VC				
	SPL			-0.296	
	EC				
	MTG	-0.474			

DP: deep pyramidal cells; SP: superficial pyramidal cells; SS: spiny stellate cells; II: inhibitory interneurons; VC: early visual cortex; SPL: superior parietal lobule; EC: entorhinal cortex; MTG: middle temporal gyrus. The posterior probability of the reported connectivities was 1.

approach would enhance our understanding of how sensory processing modulates cognitive and behavioral responses in individuals at risk for suicide.

It is important to note that our findings may contribute to the development of new treatment options for individuals at risk for suicide. While previous analyses have explored attentional bias, they have been limited in terms of offering potential therapeutic options or ways to measure the efficacy of any such options. Notably, two promising treatment methods for addressing attentional bias are attentional process training and neurofeedback. Attentional process training, such as mindfulness-based cognitive therapy, showed potential benefits in a previous study that found that mindfulness-based cognitive therapy improved Stroop Task performance in veterans at risk for suicide when responding to negative valence, suicidal, and trauma-related words (Chesin et al., 2021). However, attentional process training has not been widely applied to individuals at risk for suicide and, in addition, this type of training has shown mixed results in adults with brain injuries (Loetscher et al., 2019; Soule et al., 2025), indicating the need for more systematic and targeted approaches. Neurofeedback treatments have also shown efficacy in various populations. For example, studies have found improved brain oscillatory power in the theta and alpha bands in the frontal brain regions of healthy females with hypersensitivity and individuals with PTSD undergoing neurofeedback treatments (Hamed et al., 2022; Nicholson et al., 2023). Individuals with depression have also benefited from neurofeedback treatments, although many studies did not include HVs as controls, highlighting the need for more systematic investigation (Patil et al., 2023). Nevertheless, neurofeedback specifically involving words related to death or suicide has not been extensively explored in individuals at risk for suicide. For both attentional process training and neurofeedback treatments, improvement has primarily been estimated using behavioral changes. In contrast, the results of this study suggest that accounting for neural connectivity between the targeted brain regions responsible for sensory processing and integration could help the field evaluate the potential effectiveness of these and other methods for reducing suicide risk.

Although these preliminary findings are promising, several limitations warrant consideration. First, the relatively small sample size limits the generalizability of our results, and larger, longitudinal studies are needed to confirm these findings. Second, although comparisons are often made between those with and without suicide risk, there may be substantial variability in attentional biases among individuals at risk that are potentially influenced by the timing of suicidal thoughts. For instance, individuals with recent suicide ideation may disengage from death-related cues faster than those whose ideation occurred longer ago (Rosario-Williams et al., 2023; Rosario-Williams and Miranda, 2024). Third, participants were either medication-free or maintained on prescribed medications as clinically indicated. The heterogeneity in medication status across participants may have significantly influenced our observed neural associations, including brain connectivity patterns; future studies should examine medication-free participants or systematically control for specific medication effects to isolate the neural mechanisms of interest. Fourth, although most participants were diagnosed with major depressive disorder, symptom recurrence may have contributed to the relationship between suicide risk and neural activity, particularly in brain regions related to the default mode network (Alonso et al., 2023). Future research should investigate the heterogeneity of depressive symptomatology in the relationship between suicide risk and neural activity. Fifth, DCM was exclusively modeled in the left hemisphere to avoid interpretational and methodological complications, though this approach reduces available data. Right hemisphere DCM modeling could be used for replication in future studies. Future studies with larger sample sizes should examine bilateral networks to determine whether these connectivity patterns are hemisphere-specific or reflect general attentional bias mechanisms. Lastly, reductions in oscillatory MEG power were reported using the cluster-wise averaged effect size from key regions associated with sensory processing. However, this approach is still biased by statistical thresholding. More robust strategies, such as cross validation or the use of pre-specified brain maps derived from previous literature or public repositories, may be beneficial and should be considered in future research.

This study investigated how attentional bias and suicide risk relate to brain areas involved in processing and integrating sensory signals. The initial results indicate that individuals at risk for suicide tend to have lower activity and weaker effective connectivity in brain regions associated with sensory signal processing, especially in response to death-related cues. These findings emphasize the essential role of sensory processing mechanisms in advancing neurobiological research on suicide risk. Integrating these novel approaches into treatment plans could provide a holistic way to evaluate novel treatments for suicide risk, with important implications for clinical practice.

Data statement

The data that support the findings of this study are available from OpenNeuro (https://openneuro.org/) for the MEG data and from the National Institute of Mental Health Data Archive (NDA) (https://nda.nih.gov/) for the clinical scales.

Funding sources

This research was supported by the Intramural Research Program of the National Institutes of Health (NIH; ZIAMH002927, conducted under clinical trials NCT02543983 and NCT00397111). The contributions of

the NIH authors are considered Works of the United States Government. The findings and conclusions presented in this paper are those of the authors and do not necessarily reflect the views of the NIH or the US Department of Health and Human Services.

CRediT authorship contribution statement

Yoojin Lee: Writing – review & editing, Writing – original draft, Visualization, Investigation, Formal analysis, Conceptualization. **Jessica R. Gilbert:** Writing – review & editing, Supervision, Resources, Methodology, Investigation, Formal analysis. **Steven J. Lamontagne:** Writing – review & editing, Visualization, Conceptualization. **Halla F. Hafermann:** Writing – review & editing, Resources, Project administration, Data curation. **Laura R. Waldman:** Writing – review & editing. **Megan S. Kenna:** Writing – review & editing, Resources, Methodology, Conceptualization. **Nancy E. Adleman:** Writing – review & editing, Resources, Methodology, Conceptualization. **David A. Jobes:** Writing – review & editing, Resources, Methodology, Conceptualization. **Carlos A. Zarate Jr.:** Writing – review & editing, Supervision, Resources, Investigation, Funding acquisition. **Elizabeth D. Ballard:** Writing – review & editing, Supervision, Resources, Investigation, Funding acquisition, Conceptualization.

Declaration of competing interest

Dr. Zarate is listed as a co-inventor on a patent for the use of ketamine in major depression and suicidal ideation; as a co-inventor on a patent for the use of (2*R*,6*R*)-hydroxynorketamine, (*S*)-dehydronorketamine, and other stereoisomeric dehydroxylated and hydroxylated metabolites of (*R,S*)-ketamine in the treatment of depression and neuropathic pain; and as a co-inventor on a patent application for the use of (2*R*,6*R*)-hydroxynorketamine and (2*S*,6*S*)-hydroxynorketamine in the treatment of depression, anxiety, anhedonia, suicidal ideation, and post-traumatic stress disorder. He has assigned his patent rights to the U.S. government but will share a percentage of any royalties that may be received by the government. Dr. Jobes receives grant support from the National Institute of Mental Health (NIMH), the National Institute of Alcohol Abuse and Alcoholism (NIAAA), the Patient-Centered Outcomes Research Institute (PCORI), and the Four Pines Fund. He also receives book royalties from Gilford Press. All other authors have no conflict of interest to disclose, financial or otherwise.

Acknowledgements

The authors thank the 7SE research unit and staff for their support and Drs. Jessica Reed and Joanna Szczepanik for early contribution to the development of the task. Ioline Henter (National Institute of Mental Health) provided invaluable editorial assistance.

References

Abbassi, E., Kahlaoui, K., Wilson, M.A., Joanette, Y., 2011. Processing the emotions in words: the complementary contributions of the left and right hemispheres. Cogn. Affect. Behav. Neurosci. 11, 372–385.
Adams, R.A., Bauer, M., Pinotsis, D.A., Friston, K.J., 2016. Dynamic causal modelling of eye movements during pursuit: confirming precision-encoding in V1 using MEG. Neuroimage 132, 175–189.
Agster, K.L., Burwell, R.D., 2013. Hippocampal and subicular efferents and afferents of the perirhinal, postrhinal, and entorhinal cortices of the rat. Behav. Brain Res. 254, 50–64.
Alacreu-Crespo, A., Olie, E., Le Bars, E., Cyprien, F., Deverdun, J., Courtet, P., 2020. Prefrontal activation in suicide attempters during decision making with emotional feedback. Transl. Psychiatry 10 (1), 313.
Alahmadi, A.A.S., 2021. Investigating the sub-regions of the superior parietal cortex using functional magnetic resonance imaging connectivity. Insights Imaging 12 (1), 47.
Alonso, S., Tyborowska, A., Ikani, N., Mocking, R.J.T., Figueroa, C.A., Schene, A.H., Deco, G., Kringelbach, M.L., Cabral, J., Ruhé, H.G., 2023. Depression recurrence is accompanied by longer periods in default mode and more frequent attentional and reward processing dynamic brain-states during resting-state activity. Hum. Brain Mapp. 44, 5770–5783.
Amaral, D.G., Insausti, R., Cowan, W.M., 1983. Evidence for a direct projection from the superior temporal gyrus to the entorhinal cortex in the monkey. Brain Res. 275 (2), 263–277.
Aminoff, E.M., Kveraga, K., Bar, M., 2013. The role of the parahippocampal cortex in cognition. Trends. Cogn. Sci. 17, 379–390.
Atkinson, R.C., 1968. A proposed system and its control processes. Psychol. Learn. Motiv. 2.
Ballard Elizabeth, D., et al., 2020. Neurobiological research with suicidal participants: A framework for investigators. Gen. Hospital Psychiat. 62, 43–48. https://doi.org/10.1016/j.genhosppsych.2019.11.007.
Ballard, E.D., Ionescu, D.F., Vande Voort, J.L., Niciu, M.J., Richards, E.M., Luckenbaugh, D.A., Brutsche, N.E., Ameli, R., Furey, M.L., Zarate Jr., C.A., 2014. Improvement in suicidal ideation after ketamine infusion: relationship to reductions in depression and anxiety. J. Psychiatr. Res. 58, 161–166.
Bao, C., Zhang, Q., He, C., Zou, H., Xia, Y., Yan, R., Hua, L., Wang, X., Lu, Q., Yao, Z., 2024. Neural responses to decision-making in suicide attempters with youth major depressive disorder. Neuroimage Clin. 43, 103667.
Bastos, A.M., Usrey, W.M., Adams, R.A., Mangun, G., Fries, P., Friston, K.J., 2012. Canonical microcircuits for predictive coding. Neuron 76, 695–711.
Beck, A.T., Kovacs, M., Weissman, A., 1979. Assessment of suicidal intention: the scale for suicide ideation. J. Consult. Clin. Psychol. 47 (2), 343–352.
Becker, E.S., Strohbach, D., Rinck, M., 1999. A specific attentional bias in suicide attempters. J. Nerv. Ment. Dis. 187 (12), 730–735.
Binder, J.R., Desai, R.H., Graves, W.W., Conant, L.L., 2009. Where is the semantic system? A critical review and meta-analysis of 120 functional neuroimaging studies. Cereb. Cortex 19 (12), 2767–2796.
Brüdern, J., Spangenberg, L., Stein, M., Forkmann, T., Schreiber, D., Stengler, K., Gold, H., Glaesmer, H., 2024. Implicit measures of suicide vulnerability: investigating suicide-related information-processing biases and a deficit in behavioral impulse control in a high-risk sample and healthy controls. Behav. Res. Ther. 180, 104601.
Calvert, G.A., Thesen, T., 2004. Multisensory integration: methodological approaches and emerging principles in the human brain. J. Physiol.-Paris 98 (1–3), 191–205.
Cha, C.B., Najmi, S., Park, J.M., Finn, C.T., Nock, M.K., 2010. Attentional bias toward suicide-related stimuli predicts suicidal behavior. J. Abnorm. Psychol. 119 (3), 616–622.
Chen, C.-f., Chen, W.-n., Zhang, B., 2022. Functional alterations of the suicidal brain: a coordinate-based meta-analysis of functional imaging studies. Brain Imaging Behav. 16 (1), 291–304.
Chen, G., Saad, Z.S., Britton, J.C., Pine, D.S., Cox, R.W., 2013. Linear mixed-effects modeling approach to FMRI group analysis. Neuroimage 73, 176–190.
Chen, M.-H., Lin, W.-C., Tu, P.-C., Li, C.-T., Bai, Y.-M., Tsai, S.-J., Su, T.-P., 2019. Antidepressant and antisuicidal effects of ketamine on the functional connectivity of prefrontal cortex-related circuits in treatment-resistant depression: a double-blind, placebo-controlled, randomized, longitudinal resting fMRI study. J. Affect. Disord. 259, 15–20.
Chesin, M.S., Keilp, J.G., Kline, A., Stanley, B., Myers, C., Latorre, M., St Hill, L.M., Miller, R.B., King, A.R., Boschulte, D.R., Rodriguez, K.M., Callahan, M., Sedita, M., Interian, A., 2021. Attentional control may be modifiable with mindfulness-based cognitive therapy to prevent suicide. Behav. Brain Res. 147, 103988.
Corbetta, M., Shulman, G.L., 2002. Control of goal-directed and stimulus-driven attention in the brain. Nat. Rev. Neurosci. 3 (3), 201–215.
Correa, Á., Lupiáñez, J., Tudela, P., 2005. Attentional preparation based on temporal expectancy modulates processing at the perceptual level. Psychon. Bull. Rev. 12 (2), 328–334.
Costanza, A., Amerio, A., Aguglia, A., Magnani, L., Serafini, G., Amore, M., Merli, R., Ambrosetti, J., Bondolfi, G., Marzano, L., Berardelli, I., 2021. Hard to say, hard to understand, hard to live": possible associations between neurologic language impairments and suicide risk. Brain Sci. 11, 1594.
Cox, R.W., 1996. AFNI: software for analysis and visualization of functional magnetic resonance neuroimages. Comput. Biomed. Res. 29 (3), 162–173.
Culham, J.C., Kanwisher, N.G., 2001. Neuroimaging of cognitive functions in human parietal cortex. Curr. Opin. Psychiatry 11, 157–163.
Davies, M., 2012. Corpus of Contemporary American English (1990–2012), 9. Brigham Young University, p. 2014. Retrieved.
de Schotten, M.T., Dell'Acqua, F., Forkel, S.J., Simmons, A., Vergani, F., Murphy, D.G.M., Catani, M., 2011. A lateralized brain network for visuospatial attention. Nat. Neurosci. 14, 1245–1246.
DeVille, D.C., Kuplicki, R., Stewart, J.L., Tulsa, I., Paulus, M.P., Khalsa, S.S., 2020. Diminished responses to bodily threat and blunted interoception in suicide attempters. Elife 9.
Disner, S.G., Shumake, J.D., Beevers, C.G., 2017. Self-referential schemas and attentional bias predict severity and naturalistic course of depression symptoms. Cogn. Emot. 31 (4), 632–644.
Dixon, M.L., Dweck, C.S., 2022. The amygdala and the prefrontal cortex: the co-construction of intelligent decision-making. Psychol. Rev. 129, 1414.
Dixon-Gordon, K.L., Waite, E.E., Ammerman, B.A., Haliczer, L.A., Boudreaux, E.D., Rathlev, N., Cohen, A.L., 2022. Learning from gain and loss: links to suicide risk. J. Psychiatr. Res. 147, 126–134.
Dombrovski, A.Y., Hallquist, M.N., 2017. The decision neuroscience perspective on suicidal behavior: evidence and hypotheses. Curr. Opin. Psychiatry 30 (1), 7–14.
Dombrovski, A.Y., Hallquist, M.N., Brown, V.M., Wilson, J., Szanto, K., 2019. Value-based choice, contingency learning, and suicidal behavior in mid- and late-life depression. Biol. Psychiatry 85 (6), 506–516.

Dutriaux, L., Xu, Y., Sartorato, N., Lhuillier, S., Bottini, R., 2024. Disentangling reference frames in the neural compass. Imaging Neurosci. 2, 1–18.
First, M.B., 2002. Structured clinical interview for DSM-IV-TR axis I disorders, research version, patient edition (SCID-I/P). Biom. Res.
Gifuni, A.J., Chakravarty, M.M., Lepage, M., Ho, T.C., Geoffroy, M.C., Lacourse, E., Gotlib, I.H., Turecki, G., Renaud, J., Jollant, F., 2021. Brain cortical and subcortical morphology in adolescents with depression and a history of suicide attempt. J. Psychiatry Neurosci. 46 (3), E347–E357.
Gilbert, J.R., Galiano, C.S., Nugent, A.C., Zarate, C.A., 2021. Ketamine and attentional bias toward emotional faces: dynamic causal modeling of magnetoencephalographic connectivity in treatment-resistant depression. Front. Psychiatry 12, 673159.
Grande, X., Sauvage, M.M., Becke, A., Düzel, E., Berron, D., 2022. Transversal functional connectivity and scene-specific processing in the human entorhinal-hippocampal circuitry. Elife 11.
Gross, J., Baillet, S., Barnes, G.R., Henson, R.N., Hillebrand, A., Jensen, O., Jerbi, K., Litvak, V., Maess, B., Oostenveld, R., Parkkonen, L., Taylor, J.R., van Wassenhove, V., Wibral, M., Schoffelen, J.-M., 2013. Good practice for conducting and reporting MEG research. Neuroimage 65, 349–363.
Gutnisky, D.A., Hansen, B.J., Iliescu, B.F., Dragoi, V., 2009. Attention alters visual plasticity during exposure-based learning. Curr. Biol. 19 (7), 555–560.
Hamed, R., Mizrachi, L., Granovsky, Y., Issachar, G., Yuval-Greenberg, S., Bar-Shalita, T., 2022. Neurofeedback therapy for sensory over-responsiveness—A feasibility study. Sensors (Basel) 22, 1845.
Hamedi, A., Colborn, V.A., Bell, M., Chalker, S.A., Jobes, D.A., 2019. Attentional bias and the Suicide Status form: behavioral perseveration of written responses. Behav. Res. Ther. 120, 103403.
Hamilton, M., 1967. Development of a rating scale for primary depressive illness. Br. J. Soc. Clin. Psychol. 6 (4), 278–296.
Hansen, P., Kringelbach, M., Salmelin, R., 2010. MEG: An Introduction to Methods. Oxford Academic, New York.
Herzog, S., Keilp, J.G., Galfalvy, H., Mann, J.J., Stanley, B.H., 2023. Attentional control deficits and suicidal ideation variability: an ecological momentary assessment study in major depression. J. Affect. Disord. 323, 819–825.
Hillebrand, A., Singh, K.D., Holliday, I.E., Furlong, P.L., Barnes, G.R., 2005. A new approach to neuroimaging with magnetoencephalography. Hum. Brain Mapp. 25 (2), 199–211.
Hipp, J.F., Hawellek, D.J., Corbetta, M., Siegel, M., Engel, A.K., 2012. Large-scale cortical correlation structure of spontaneous oscillatory activity. Nat. Neurosci. 15, 884–890.
Hopfinger, J.B., Buonocore, M.H., Mangun, G.R., 2000. The neural mechanisms of top-down attentional control. Nat. Neurosci. 3, 284–291.
Hunter, A.M., Leuchter, A.F., Cook, I.A., Abrams, M., 2010. Brain functional changes (QEEG cordance) and worsening suicidal ideation and mood symptoms during antidepressant treatment. Acta Psychiatr. Scand. 122, 461–469.
Jagger-Rickels, A., Stumps, A., Rothlein, D., Evans, T., Lee, D., McGlinchey, R., DeGutis, J., Esterman, M., 2023. Aberrant connectivity in the right amygdala and right middle temporal gyrus before and after a suicide attempt: examining markers of suicide risk. J. Affect. Disord. 335, 24–35.
John, Y.J., Zikopoulos, B., Bullock, D., Barbas, H., 2016. The emotional gatekeeper: a computational model of attentional selection and suppression through the pathway from the amygdala to the inhibitory thalamic reticular nucleus. PLoS. Comput. Biol. 12 (2), e1004722.
Keilp, J.G., Gorlyn, M., Oquendo, M.A., Burke, A.K., Mann, J.J., 2008. Attention deficit in depressed suicide attempters. Psychiatry Res. 159 (1–2), 7–17.
Kerr, K.M., Agster, K.L., Furtak, S.C., Burwell, R.D., 2007. Functional neuroanatomy of the parahippocampal region: the lateral and medial entorhinal areas. Hippocampus 17, 697–708.
Kim, D.J., Bartlett, E.A., DeLorenzo, C., Parsey, R.V., Kilts, C., Cáceda, R., 2021. Examination of structural brain changes in recent suicidal behavior. Psychiatry Res.: Neuroimaging 307, 111216.
Lamontagne, S.J., Zabala, P.K., Zarate Jr., C.A., Ballard, E.D., 2023. Toward objective characterizations of suicide risk: a narrative review of laboratory-based cognitive and behavioral tasks. Neurosci. Biobehav. Rev. 153, 105361.
Large, M.M., 2018. The role of prediction in suicide prevention. Dialogues. Clin. Neurosci. 20 (3), 197–205.
Lee, Y., Gilbert, J.R., Waldman, L.R., Zarate Jr., C.A., Ballard, E.D., 2024. Potential association between suicide risk, aggression, impulsivity, and the somatosensory system. Soc. Cogn. Affect. Neurosci. 19, nsae041.
Li, L., Griffiths, M.D., Mei, S., Niu, Z., 2021. The mediating role of impulsivity and the moderating role of gender between fear of missing out and gaming disorder among a sample of Chinese University students. Cyberpsychol. Behav. Soc. Netw. 24 (8), 550–557.
Loetscher, T., Potter, K.-J., Wong, D., das Nair, R., 2019. Cognitive rehabilitation for attention deficits following stroke. Cochrane Database Syst. Rev. 2019, CD002842.
Luo, W., Feng, W., He, W., Wang, N.Y., Luo, Y.J., 2010. Three stages of facial expression processing: ERP study with rapid serial visual presentation. Neuroimage 49, 1857–1867.
Madsen, T., Erlangsen, A., Nordentoft, M., 2017. Risk estimates and Risk factors related to psychiatric inpatient suicide-an overview. Int. J. Environ. Res. Public Health 14 (3).
Maier, W., Buller, R., Philipp, M., Heuser, I., 1988. The Hamilton Anxiety Scale: reliability, validity and sensitivity to change in anxiety and depressive disorders. J. Affect. Disord. 14 (1), 61–68.
Malone, T.J., Tien, N.W., Ma, Y., Cui, L., Lyu, S., Wang, G., Nguyen, D., Zhang, K., Myroshnychenko, M.V., Tyan, J., Gordon, J.A., Kupferschmidt, D.A., Gu, Y., 2023. A consistent map in the medial entorhinal cortex supports spatial memory. bioRxiv.
Mandel, A.A., Mitchell, E., Krush, C., Revzina, O., 2025. Differences in suicide-specific attentional bias based on stimuli across the suicide stroop and disengagement tasks. J. Affect. Disord. 369, 87–94.
Meneghetti, C., Ronconi, L., Pazzaglia, F., De Beni, R., 2014. Spatial mental representations derived from spatial descriptions: the predicting and mediating roles of spatial preferences, strategies, and abilities. Br. J. Psychol. 105 (3), 295–315.
Monroe, J.F., Griffin, M., Pinkham, A., Loughead, J., Gur, R.C., Roberts, T.P.L., Edgar, J. C., 2013. The fusiform response to faces: explicit versus implicit processing of emotion. Hum. Brain Mapp. 34, 1–11.
Montgomery, S.A., Asberg, M., 1979. A new depression scale designed to be sensitive to change. Br. J. Psychiatry 134, 382–389.
Murai, Y., Whitney, D., 2021. Serial dependence revealed in history-dependent perceptual templates. Curr. Biol. 31 (14), e3183.
Nicholson, A.A., Densmore, M., Frewen, P.A., Neufeld, R.W.J., Théberge, J., Jetly, R., Lanius, R.A., Ros, T., 2023. Homeostatic normalization of alpha brain rhythms within the default-mode network and reduced symptoms in post-traumatic stress disorder following a randomized controlled trial of electroencephalogram neurofeedback. Brain Commun. 5, fcad068.
Nock, M.K., Park, J.M., Finn, C.T., Deliberto, T.L., Dour, H.J., Banaji, M.R., 2010. Measuring the suicidal mind: implicit cognition predicts suicidal behavior. Psychol. Sci. 21 (4), 511–517.
Öğüt, Ç., Başar, K., Karahan, S., 2023. Impulsivity in depression: its relation to suicidality. J. Psychiatr. Pract. 29 (3), 189–201.
Olié, E., Ding, Y., Le Bars, E., de Champfleur, N.M., Mura, T., Bonafé, A., Courtet, P., Jollant, F., 2015. Processing of decision-making and social threat in patients with history of suicidal attempt: a neuroimaging replication study. Psychiatry Res. 234 (3), 369–377.
Ostrowski, J., Rose, M., 2024. Increases in pre-stimulus theta and alpha oscillations precede successful encoding of crossmodal associations. Sci. Rep. 14, 7895.
Parisi, S., Gunasekara, R., Canale, C., Hasta, F., Azizi, H., 2021. The role of the anterior cingulate cortex and insular cortex in suicidal memory and intent. Cureus 13 (7).
Patil, A.U., Lin, C., Lee, S.-H., Huang, H.-W., Wu, S.-C., Madathil, D., Huang, C.-M., 2023. Review of EEG-based neurofeedback as a therapeutic intervention to treat depression. Psychiatry Res. Neuroimaging 329, 111591.
Patten, M.L., Mannion, D.J., Clifford, C.W., 2017. Correlates of perceptual orientation biases in human primary visual cortex. J. Neurosci. 37 (18), 4744–4750.
Peckham, A.D., McHugh, R.K., Otto, M.W., 2010. A meta-analysis of the magnitude of biased attention in depression. Depress. Anxiety. 27 (12), 1135–1142.
Peng, H., Wu, K., Li, J., Qi, H., Guo, S., Chi, M., Wu, X., Guo, Y., Yang, Y., Ning, Y., 2014. Increased suicide attempts in young depressed patients with abnormal temporal–parietal–limbic gray matter volume. J. Affect. Disord. 165, 69–73.
Petzschner, F.H., Garfinkel, S.N., Paulus, M.P., Koch, C., Khalsa, S.S., 2021. Computational models of interoception and body regulation. Trends. Neurosci. 44 (1), 63–76.
Petzschner, F.H., Weber, L.A.E., Gard, T., Stephan, K.E., 2017. Computational psychosomatics and Computational Psychiatry: toward a joint framework for differential diagnosis. Biol. Psychiatry 82 (6), 421–430.
Peyk, P., Schupp, H.T., Elbert, T., Junghöfer, M., 2008. Emotion processing in the visual brain: a MEG analysis. Brain Topogr. 20, 205–215.
Pinotsis, D.A., Schwarzkopf, D.S., Litvak, V., Rees, G., Barnes, G., Friston, K.J., 2013. Dynamic causal modelling of lateral interactions in the visual cortex. Neuroimage 66, 563–576.
Reagh, Z.M., Yassa, M.A., 2014. Object and spatial mnemonic interference differentially engage lateral and medial entorhinal cortex in humans. Proc. Natl. Acad. Sci. U. S. A. 111 (40), E4264–E4273.
Reed, J.L., Nugent, A.C., Furey, M.L., Szczepanik, J.E., Evans, J.W., Zarate Jr, C.A., 2018. Ketamine normalizes brain activity during emotionally valenced attentional processing in depression. NeuroImage: Clin. 20, 92–101.
Richard-Devantoy, S., Ding, Y., Turecki, G., Jollant, F., 2016. Attentional bias toward suicide-relevant information in suicide attempters: a cross-sectional study and a meta-analysis. J. Affect. Disord. 196, 101–108.
Risch, N., Dupuis-Maurin, K., Dubois, J., Courtet, P., Olié, E., 2023. Sensitivity to ostracism is blunted in suicide attempters only when they report suicidal ideation. J. Affect. Disord. 337, 169–174.
Rogers, M.L., Carosa, C.L., Haliczer, L.A., Hughes, C.D., Schofield, C.A., Armey, M.F., 2023. The suicide dot probe task: psychometric properties and validity in relation to suicide-related outcomes. Suicide Life Threat. Behav. 53 (6), 1010–1024.
Rolls, E.T., Deco, G., Huang, C.-C., Feng, J., 2023. Multiple cortical visual streams in humans. Cereb. Cortex 33 (7), 3319–3349.
Rosario-Williams, B., Akter, S., Kaur, S., Mirada, R., 2023. Suicide-related construct accessibility and attention disengagement bias in suicide ideation. J. Psychopathol. Clin. Sci. 132 (2), 173–184.
Rosario-Williams, B., Miranda, R., 2024. Negative affect influences suicide-specific attentional biases. J. Mood Anxiety Disord. 7.
Ryan, E.P., Oquendo, M.A., 2020. Suicide risk assessment and prevention: challenges and opportunities. Focus (Am. Psychiatr. Publ.) 18 (2), 88–99.
Schmaal, L., van Harmelen, A.L., Chatzi, V., Lippard, E.T.C., Toenders, Y.J., Averill, L.A., Mazure, C.M., Blumberg, H.P., 2020. Imaging suicidal thoughts and behaviors: a comprehensive review of 2 decades of neuroimaging studies. Mol. Psychiatry 25 (2), 408–427.
Schofield, C.A., Johnson, A.L., Inhoff, A.W., Coles, M.E., 2012. Social anxiety and difficulty disengaging threat: evidence from eye-tracking. Cogn. Emot. 26 (2), 300–311.
Schrooten, M., Ghumare, E.G., Seynaeve, L., Theys, T., Dupont, P., Van Paesschen, W., Vandenberghe, R., 2017. Electrocorticography of spatial shifting and attentional selection in human superior parietal cortex. Front. Hum. Neurosci. 11, 240.

Schurz, M., Radua, J., Aichhorn, M., Richlan, F., Perner, J., 2014. Fractionating theory of mind: a meta-analysis of functional brain imaging studies. Neurosci. Biobehav. Rev. 42, 9–34.
Sequeira, S.L., Rosen, D.K., Silk, J.S., Hutchinson, E., Allen, K.B., Jones, N.P., Price, R.B., Ladouceur, C.D., 2021. Don't judge me!": links between in vivo attention bias toward a potentially critical judge and fronto-amygdala functional connectivity during rejection in adolescent girls. Dev. Cogn. Neurosci. 49, 100960.
Seth, A.K., Friston, K.J., 2016. Active interoceptive inference and the emotional brain. Philos. Trans. R Soc. L. B Biol. Sci. 371 (1708).
Smith, A.R., Duffy, M.E., Joiner, T.E., 2021. Introduction to the special issue on interoception and suicidality. Behav. Ther. 52 (5), 1031–1034.
Snijders, T.M., Petersson, K.M., Hagoort, P., 2010. Effective connectivity of cortical and subcortical regions during unification of sentence structure. Neuroimage 52 (4), 1633–1644.
Soule, A.C., Fish, T.J., Thomas, K.G.F., Schrieff-Brown, L., 2025. Attention training following moderate to severe traumatic brain injury in adults: a systematic review. Arch. Phys. Med. Rehabil. 106, 433–443.
Stephan, K.E., Manjaly, Z.M., Mathys, C.D., Weber, L.A., Paliwal, S., Gard, T., Tittgemeyer, M., Fleming, S.M., Haker, H., Seth, A.K., 2016. Allostatic self-efficacy: a metacognitive theory of dyshomeostasis-induced fatigue and depression. Front. Hum. Neurosci. 10, 550.
Stephan, K.E., Penny, W.D., Moran, R.J., den Ouden, H.E., Daunizeau, J., Friston, K.J., 2010. Ten simple rules for dynamic causal modeling. Neuroimage 49 (4), 3099–3109.
Substance Abuse and Mental Health Services Administration, 2024. Key Substance Use and Mental Health Indicators in the United States: Results from the 2023 National Survey On Drug Use and Health (HHS Publication No. PEP24-07-021, NSDUH Series H-59). Center for Behavioral Health Statistics and Quality, Substance Abuse and Mental Health Services Administration, Rockville, MD. Available at: https://www.samhsa.gov/data/report/2023-nsduh-annual-national-report.
Tavakoli, P., Jerome, E., Boafo, A., Campbell, K., 2021. Attentional bias deficits in adolescent suicide attempters during an emotional Stroop task: an ERP study. Front. Psychiatry 12, 694147.
Thompson, C., Ong, E.L.C., 2018. The association between suicidal behavior, attentional control, and frontal asymmetry. Front. Psychiatry 9, 79.
Toll, R.T., Wu, W., Naparstek, S., Zhang, Y., Naryan, M., Patenaude, B., De Los Angeles, C., Sarhadi, K., Anicetti, N., Longwell, P., Shpigel, E., Wright, R., Newman, J., Gonzalez, B., Hart, R., Mann, S., Abu-Amara, D., Sarhadi, K., Cornelssen, C., Marmar, C., Etkin, A., 2020. An electroencephalography connectomic profile of posttraumatic stress disorder. Am. J. Psychiatry 177, 233–243.
Tong, F., 2003. Primary visual cortex and visual awareness. Nat. Rev. Neurosci. 4, 219–229.
Toussaint, B., Heinzle, J., Stephan, K.E., 2024. A computationally informed distinction of interoception and exteroception. Neurosci. Biobehav. Rev., 105608
Trapp, W., Kalzendorf, C., Baum, C., Hajak, G., Lautenbacher, S., 2018. Attentional biases in patients suffering from unipolar depression: results of a dot probe task investigation. Psychiatry Res. 261, 325–331.
Tsypes, A., Owens, M., Gibb, B.E., 2017. Suicidal ideation and attentional biases in children: an eye-tracking study. J. Affect. Disord. 222, 133–137.
Tsypes, A., Szanto, K., Bridge, J.A., Brown, V.M., Keilp, J.G., Dombrovski, A.Y., 2022. Delay discounting in suicidal behavior: myopic preference or inconsistent valuation? J. Psychopathol. Clin. Sci. 131 (1), 34–44.
Tzourio, N., El Massioui, F., Crivello, F., Joliot, M., Renault, B., Mazoyer, B., 1997. Functional anatomy of human auditory attention studied with PET. Neuroimage 5 (1), 63–77.
Wang, H.-Y., Zhang, L., Guan, B.-Y., Wang, S.-Y., Zhang, C.-H., Ni, M.-F., Miao, Y.-W., Zhang, B.-W., 2024. Resting-state cortico-limbic functional connectivity pattern in panic disorder: relationships with emotion regulation strategy use and symptom severity. J. Psychiatr. Res. 169, 97–104.
Wang, L., Zhao, Y., Edmiston, E.K., Womer, F.Y., Zhang, R., Zhao, P., Jiang, X., Wu, F., Kong, L., Zhou, Y., Tang, Y., Wei, S., 2019. Structural and functional abnormities of amygdala and prefrontal cortex in major depressive disorder with suicide attempts. Front. Psychiatry 10, 923.
Warriner, A.B., Kuperman, V., Brysbaert, M., 2013. Norms of valence, arousal, and dominance for 13,915 English lemmas. Behav. Res. Methods 45, 1191–1207.
Wessing, I., Romer, G., Junghöfer, M., 2017. Hypervigilance-avoidance in children with anxiety disorders: magnetoencephalographic evidence. J. Child Psychol. Psychiatry 58, 103–112.
WHO, 2021. Suicide worldwide in 2019: global health estimates. Geneva: world Health Organization. Licence: CC BY-NC-SA 3.0 IGO.
Yaniv, D., Vouimba, R.M., Diamond, D.M., Richter-Levin, G., 2003. Simultaneous induction of long-term potentiation in the hippocampus and the amygdala by entorhinal cortex activation: mechanistic and temporal profiles. Neuroscience 120 (4), 1125–1135.
Zeidman, P., Jafarian, A., Seghier, M.L., Litvak, V., Cagnan, H., Price, C.J., Friston, K.J., 2019. A guide to group effective connectivity analysis, part 2: second level analysis with PEB. Neuroimage 200, 12–25.
Zikopoulos, B., Barbas, H., 2012. Pathways for emotions and attention converge on the thalamic reticular nucleus in primates. J. Neurosci. 32 (15), 5338–5350.